修士論文

Master Thesis

Force Sensorless Power Assist Control for Wheelchairs Based on Human Intention Extraction
（人間の意図抽出に基づく車椅子の フォースセンサレスパワーアシスト制御）

指導教員　堀　洋一 教授
Advisory Professor　Yoichi HORI

平成 28 年 2 月 4 日提出
February 4, 2016

東京大学大学院 工学系研究科 電気系工学専攻
Department of Electrical Engineering and Information Systems, The University of Tokyo
37–146888
喜　楽楽
Lele XI

Abstract

Mobility is one of the basic requirements of human. During the last 100 years, wheelchair was one of the important devices to assist handicapped people to regain some mobility. Antique wheelchair propelled manually has helped thousands of handicapped people to regain some mobility. Recently, modern battery powered wheelchairs have also increased the range of activities of the users.

Basically, the wheelchairs can be divided into three main categories by considering the operating levels: Manual Wheelchair, Power Assist Wheelchair (PAW), Electric Wheelchair (EW). The wheelchair allows handicapped people to move at long distance. However, propelling a manual wheelchair for a long time may cause pain in the arms. On contrast, using EW all day long cannot achieve the effect of exercising upper limbs. Therefore, the market demand for PAW has increased continuously since the users can drive the PAW with less physiologic and biomechanical effort.

As a human-machine system, it is important for PAW to sense the human force and operation. Generally speaking, PAW has two independent wheels, in which two in-wheel motors are installed. There is a force sensor in each handrim to detect human force. Therefore, the assist torque can be offered by each in-wheel motor using the information from the force sensors.

However, force sensors are heavy and expensive. Moreover, force sensors can only detect force when the force is just applied on it which means it is difficult to use force sensors in the caregiver type. In this paper, a disturbance observer (DOB) based force estimator is used to estimate human force instead of force sensors. However, DOB based force estimator can only detect the external force including the disturbance, therefore, it is important to separate human force and the disturbance to guarantee the operability of the overall system.

In the previous research, the Viscous and Coulomb friction model is used to compensate the friction force. However, when the wheelchairs are changing its directions, the sliding force from casters will have a large effect on the overall system. It is difficult to compensate the sliding force without knowing the information of caster orientation. In this paper, a caster orientation observer is applied to detect the movement of the casters firstly. Then the sliding resistance is compensated.

Another problem is the viscous coefficient and the coulomb coefficient need to be modeled

beforehand. This makes the force sensorless difficult to be realized. In this paper, a Recursive Least Square (RLS) with multiple forgetting method is used to estimate human force and the friction force simultaneously. Using the proposed method, it will not be necessary to model friction force beforehand. Furthermore, since the friction coefficient can also be estimated by using the proposed method, the assist rate can be adjusted in different environments.

In this paper, a method to estimate human input timing is also developed. Using this method, the human intention can be extracted with the condition that disturbance changes much slower than human input.

All proposed methods are demonstrated by the simulation and experimental results.

Contents

Contents of Figure

Contents of Table

Chapter 1

Introduction

1.1 The Necessity of Wheelchairs

According to statistical results from Ministry of Health, Labour and Welfare (MHLW) in 2009, the population over 65 years old in Japan is already up to 20%. 30% of them need care-givers to take care of their life. Furthermore, about 2.6% of the total population is handicapped, and 67% of them use wheelchairs as assist devices. In 2035, the population over 65 years old in Japan will be more than 33%[1]. That means more than ten million people in Japan are using wheelchairs , or need ones near future.

During the last 100 years, wheelchair has played an important role in assisting handicapped people to regain some mobility. Manual wheelchair has helped thousands of handicapped people to regain some mobility. Recently, modern battery powered wheelchairs such as power assist wheelchair and electric wheelchair have also increased the range of activities of the users.

In Japan, according to [3], the annual sales for Manual Wheelchair begin to reduce since 2005. On contrast, the annual sales for Electric Wheelchair (EW) has been 7 thousand since 2004. It can be inferred that more people are using EW to regain some mobility.

Table 1: Annual sales for welfare vehicles[3]

Year	1999	2000	2001	2002	2003	2004	2005	2006
Manual Wheelchair (thousand)	428	406	393	397	375	388	365	358
Electric Wheelchair (thousand)	6	9	7	6	6	7	7	7
Welfare Vehicles (thousand)	22	26	30	33	38	37	37	35

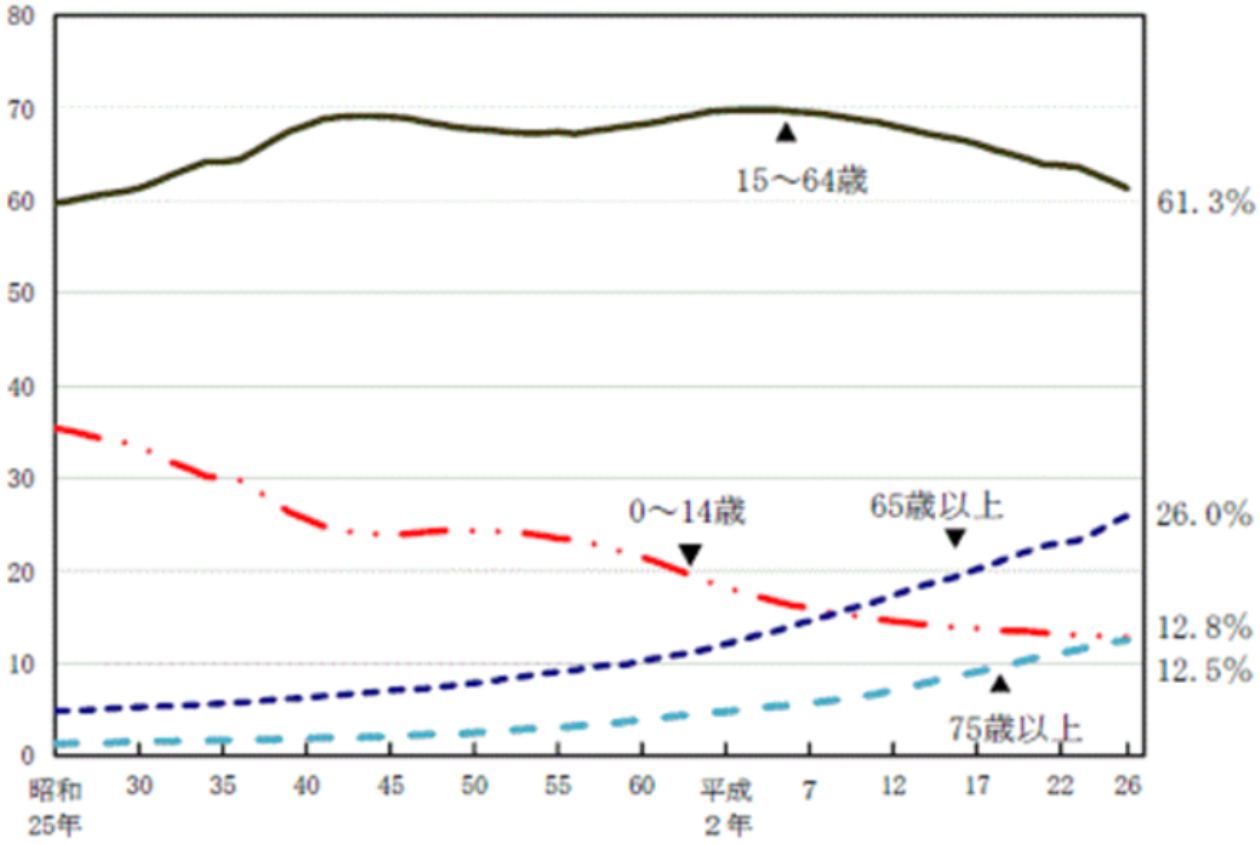

Figure 1: The population over 65 years in Japan[2]

1.2 The Categories of Wheelchairs

The wheelchairs can be divided into three main categories by considering the operating levels: Manual Wheelchair, Power Assist Wheelchair (PAW) and Electric Wheelchair (EW).

Manual wheelchairs have some advantages. It is lighter and cheaper when comparing with PAW and EW and it is easy to carry to a new place by cars. However, people have to use their own force to drive a manual wheelchair. Propelling a manual wheelchair for a long time may cause pain in the arms [4].

PAW has two independent driving wheels with two in-wheel motors installed. There is a force sensor in each handrim to detect the human force respectively. Therefore, the assist torque can be offered by each in-wheel motor using the information from the torque sensors. PAW has the advantages of effort-saving and good mobility[5]. People can drive the PAW with their own strength but with less physiologic and biomechanical effort. Most of the PAWs can be split into several parts, that makes PAW also easy to be carry out to a new place.

The driving force from EW is totally from motors. Users can drive the EW through some input device. EW is quite heavy compared with Manual Wheelchair and PAW. However, it almost takes no effort from users.

(a) Manual Wheelchair (Care-Tec Japan, CAH-50SU)

(b) Power Assist Wheelchair (YAMAHA, JWX-2)

(c) Electric Wheelchair (NISSIN, Patrafour)

In this paper, the research is concentrated on PAW.

1.3 Research Trends of Power Assist Wheelchair

“ Power assist control ” is considered to be one of the important technologies for intelligent assist robots. This technology makes it possible for a user to drive a wheelchair with less effort. The force from users can be enlarged by each in-wheel motors in each wheel.

PAW has the advantages of effort-saving and good mobility. Such system involves a full human-machine interaction which requires good performance in different conditions. Various kinds of technologies are developed. For instance, Oh *et al*. proposed an Integrated Motion Control (IMC) method to control the PAW in the longitudinal, lateral, and the pitch directions independently [6]. K.Kim proposed Yaw Motion Control for PAW under lateral disturbance environments[7][8], aiming to remove the influence from the lateral disturbance. Seki *et al*. proposed a safety driving control for PAW based on regenerative brake[9]. When the velocity of the wheelchair increases on the slope, this control system will switch from “ driving mode ”to “ braking mode ”. Shibata and Murakami proposed Repulsive Compliance Control in pushing tasks [10], this makes users easy to carry out pushing task. Tashiro and Murakami proposed a step passage control for PAW to passing over steps[11]. In [10] and [11], a disturbance observer (DOB) based force estimator [12] is used to detect human force instead of torque sensors.

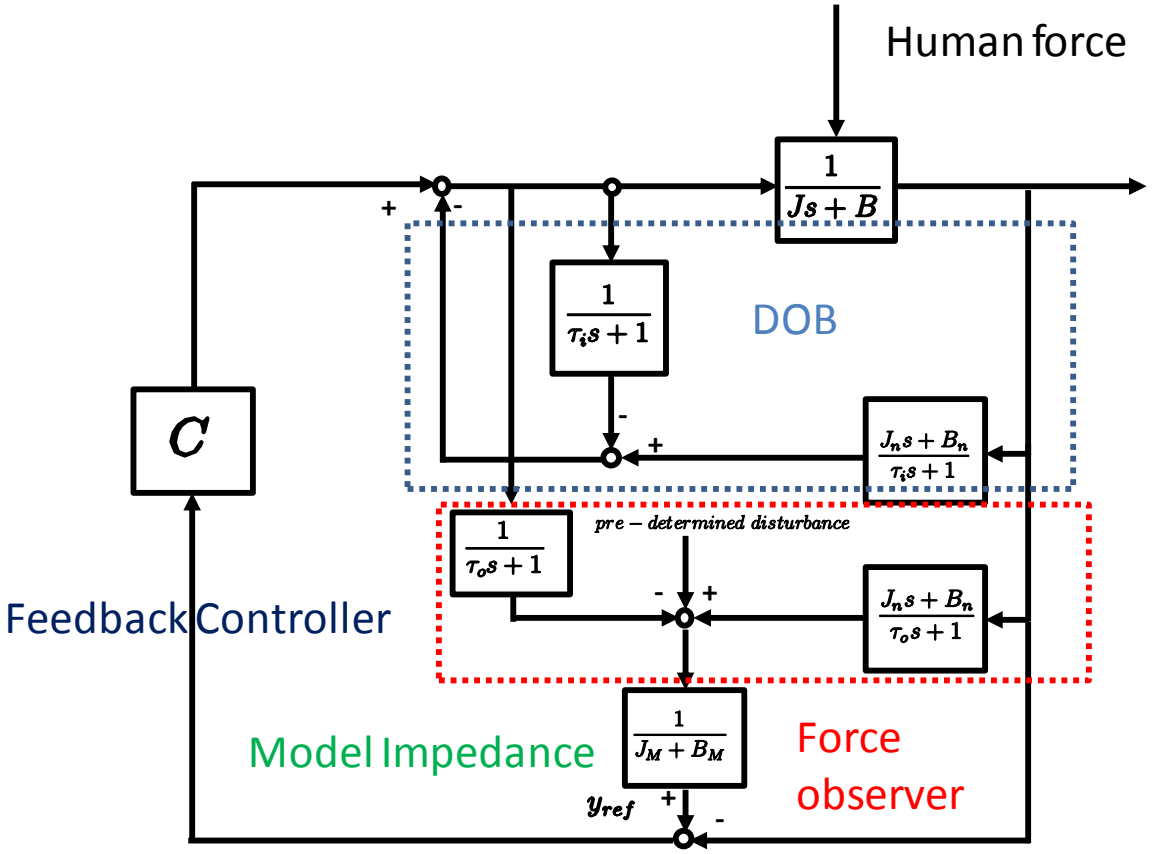

Figure 2: Structure of FSPAC

1.4 Force Sensorless Power Assist Control and Its Application on PAW

1.4.1 Force Sensorless Power Assist Control

The force control has drawn more intention than ever especially due to the recent trend of the human-machine system to human life support. However, force sensors make these systems heavy and expensive. Force Sensorless Power Assist Control (FSPAC) which only use encoders have solved the problem. Due to the simplicity and low cost, FSPAC has become one of the most important technologies in human-machine systems. In [10] and [11], a disturbance observer (DOB) [12] based force estimator is used to detect human force to substitute force sensors in PAW. In [13], Vision-based Reaction Force Observer algorithm is used in the power assist opening door system.

The general structure of FSPAC is shown in Figure 2[14][15]. J and B are the actual inertia and damping of the plant, J_n and B_n are the nominal inertia and damping for DOB and the

DOB based force estimator. J_M and B_M stand for the model inertia and damping of the model impedance. τ_i and τ_o represent the time constant for DOB and DOB based force estimator, respectively.

The entire structure can be divided into four parts: a disturbance observer, a DOB based force estimator, model impedance control and a feedback control. The disturbance observer here aims to reject the lumped disturbance which include some disturbance such as the gravity force and the friction force. Noticing that the gravity force and the friction force among the lumped disturbance should be compensated beforehand when use DOB based force estimator to guarantee the assist torque only given to the human force.

The model impedance control part decides how large the assist torque will be. Combining the feedback control loop, the reference y_{ref} will be tracked. The impedance can be adjusted according to the users' feeling.

The model impedance can be expressed as a transfer function from the external force to velocity reference. The model impedance J_M and B_M should be set as $J_M < J$ and $B_M < J$ so the users will feel less impedance.

Finally, the controller C determines the tracking characteristics.

1.4.2 The application on PAW

In [10], [11] and [16], FSPAC method is used in PAW. However, there are still some problems remained to be solved. Firstly, the gravity force and the friction force among the lumped disturbance should be compensated beforehand, this means the system can only be used in a certain environment. When the environment changes, the disturbance should be modeled again.

Secondly, the Viscous and Coulomb friction model shown in Figure 3 is often used to compensate for the friction force. However, in real systems, many other disturbance such as sliding resistance from casters and disturbance from axles may have a large effect on the system. It is hard to say that the human input can be obtained by subtracting this modeled disturbance from the external force.

1.5 Human Force Extraction

In this paper, human force can be separated by two ways. The first one is to model the disturbance as correct as possible, since the entire input is known, the human input can be obtained by removing the modeled disturbance. The second method is to use different characteristics of human force and the disturbance force to extract human intention. For example,

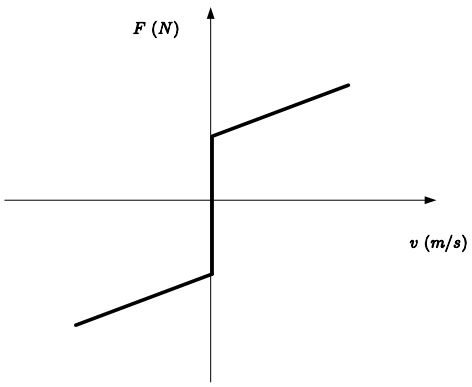

(a) Normal type.

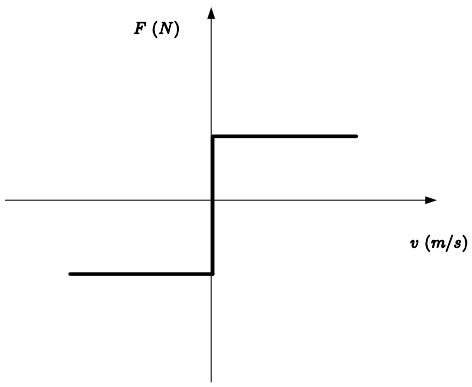

(b) Type when Viscous part is neglected.

Figure 3: Viscous and Coulomb friction model

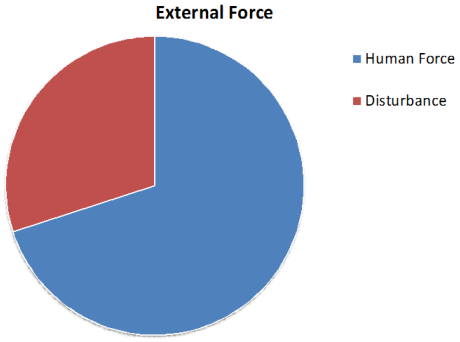

(a) Modeling the disturbance.

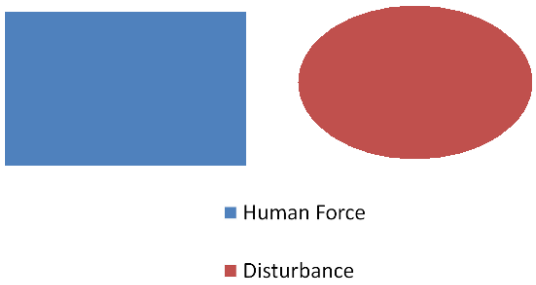

(b) Using different characteristics.

Figure 4: Human force extraction

the human input for manual wheelchairs show its feature in the frequency domain [17][18], this information can be used to obtain human input.

Figure 4 show the principles of this two methods.

1.6 The Purpose of this Research

The research aim for this paper is to extract human force on PAW without force sensors .

DOB based force estimator is firstly used in the system to extract external force. However, disturbance is also included in the external force. In a human-machine system, the power assist force should just be given to the human force. In this paper, three methods are proposed to get human force (human input timing). Simulation and experimental results show the validity of the two proposed method.

In this paper, the application is PAW. The author believe similar method can be used in other human-machine systems.

1.7 The Structure of the Paper

Figure 5 shows the entire structure of this paper.

In Chapter two, PAW is modeled considering the lateral and longitudinal directions. This is because users will feel different in the lateral and longitudinal directions. And the control system can be designed independently for lateral and longitudinal directions.

In Chapter three, the entire FSPAC system and the details for experimental devices are introduced.

In Chapter four, human force is estimated by compensating the sliding force from casters.

In Chapter five, the multiple forgetting RLS based method to separate human force and friction force will be discussed. Using this method, the compensation beforehand will not be needed.

In Chapter six, a method to estimate human input timing is introduced. Finally, the conclusion will be shown in Chapter seven.

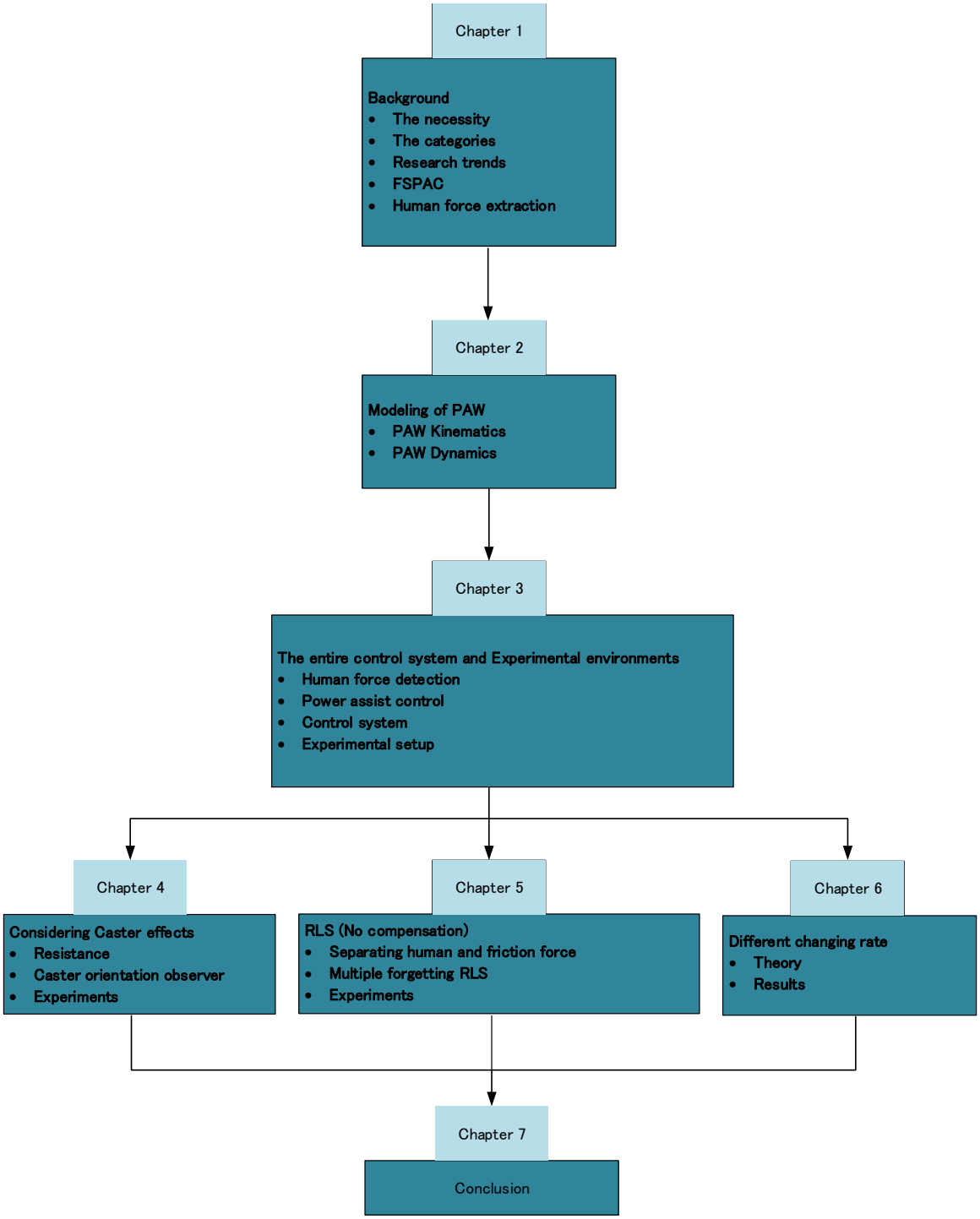

Figure 5: The configuration of this paper

Chapter 2

Dynamic Modeling of PAW by Considering the Longitudinal and the Lateral Directions

In this chapter, the modeling method for PAW will be discussed.

2.1 PAW Kinematics

A power assist wheelchair has two independent electric in-wheel motors. Figure 6 shows a schematic of a wheelchair. In this paper, three assumptions are set

- The weight of the person and the wheelchair is symmetrical.
- Slip between the road and the wheels can be neglected.
- The wheelchair will not move in the pitch direction which means the casters will not leave the road.

Most wheelchairs are designed in a symmetrical way and the weight of the person are considered to be symmetrical too. Since the wheelchair is always move in a low speed, the slips between tire and road can also be neglected. An assist limitation will also be set to prevent over turning.

There are two basic motions for wheelchairs, the straight motion and the rotational motion. Here, ω_S means the angular velocity of the straight motion, ω_Y means the angular velocity of the rotational (yaw) motion, and ω_R and ω_L represent the angular velocity of the right and the left wheel, respectively. ω_S and the ω_Y can be written as

$$\omega_S = (\omega_R + \omega_L)/2, \tag{2-1}$$

$$\omega_Y = (\omega_R - \omega_L)/2. \tag{2-2}$$

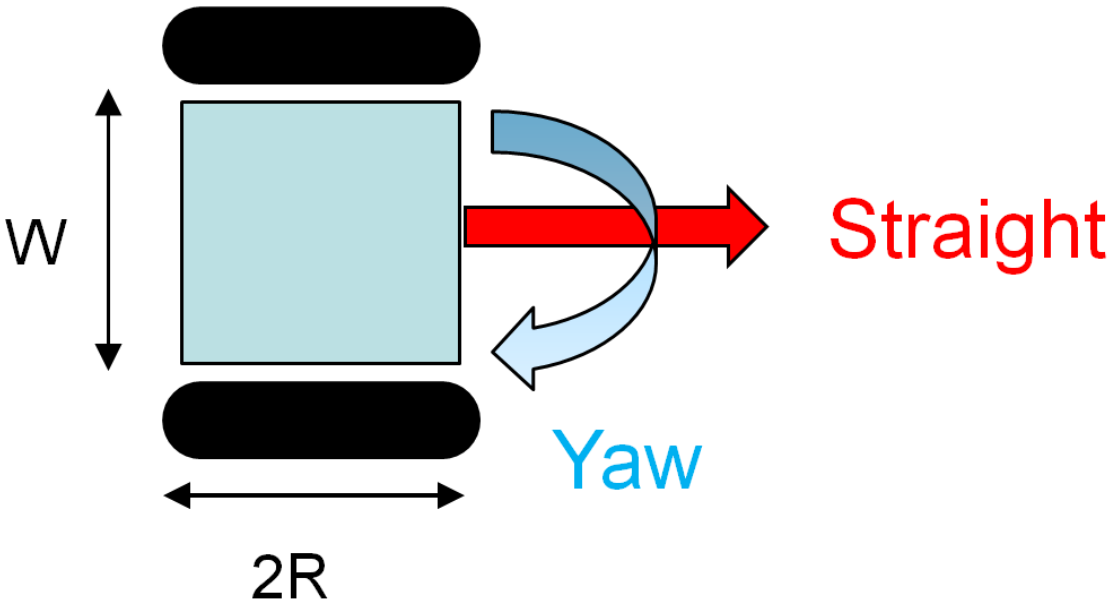

s

Figure 6: The basic structure of a wheelchair

The equation 2-1 and 2-2 can be used not only for the velocity but also the angular information, input torque, the motor torque, and the disturbance from each side. A matrix can be used here to explain the transformation.

$$\begin{bmatrix} \omega_S \\ \omega_Y \end{bmatrix} = \begin{bmatrix} 1/2 & 1/2 \\ 1/2 & -1/2 \end{bmatrix} \begin{bmatrix} \omega_R \\ \omega_L \end{bmatrix}. \tag{2-3}$$

2.2 PAW Dynamics

The linear velocity of the straight motion and the yaw rotation speed can be written as :

$$v_S = R\omega_S, \gamma = \frac{2R}{W}\omega_Y. \tag{2-4}$$

R and W are the radius of the driven wheel and the width of the wheelchair, respectively, as shown in Figure 6. The motion of wheelchair (+human) can be divided into four parts−−the entire straight motion, the entire rotational motion, the left wheel motion, the right wheel motion. These four motions can be written as below:

$$M_{v_s}\dot{v}_s + D_{vs}v = F_L + F_R + d_{v_s}, \tag{2-5}$$

$$J_\gamma\dot{\gamma} + B_\gamma\gamma = \frac{W}{2}(-F_L + F_R) + d_\gamma, \tag{2-6}$$

$$J_w\dot{\omega}_R + B_w\omega_R = \tau_R - f_R + d_{wR}, \tag{2-7}$$

$$J_w\dot{\omega}_L + B_w\omega_L = \tau_L - f_L + d_{wL}. \tag{2-8}$$

Here, M_v and D_v represent the total mass and damping coefficient, respectively. F_R,F_L and d_{v_s},d_γ are the driving force of each side and disturbance of the straight and yaw motion. f_L

and f_R represent the friction force of each side. τ_L and τ_R means input torque, d_{wR} and d_{wL} are the disturbance except friction force of each side. J_γ and J_ω stand for the inertia of the yaw motion and the wheel. The B_γ and B_ω are viscous coefficients of yaw motion and wheel, respectively. Based on the equation 2-1, 2-2, 2-5 to 2-8, we can get a dynamic function only relate to the two rear wheels.

$$J_S\dot{\omega}_S + B_S\omega_S = \tau_S + d_S, \tag{2-9}$$

$$J_Y\dot{\omega}_Y + B_Y\omega_Y = \tau_Y + d_Y. \tag{2-10}$$

Where

$$J_S = J_\omega + \frac{1}{2}M_v R^2, \tag{2-11}$$

$$J_Y = J_\omega + \frac{1}{2}J_\gamma(\frac{2R}{W})^2, \tag{2-12}$$

$$B_S = B_\omega + \frac{1}{2}D_v R^2, \tag{2-13}$$

$$B_Y = B_\omega + \frac{1}{2}B_\gamma(\frac{2R}{W})^2 \tag{2-14}$$

$$\tau_S = \frac{\tau_R + \tau_L}{2} \tag{2-15}$$

$$\tau_Y = \frac{\tau_R - \tau_L}{2}. \tag{2-16}$$

Here, J_S and J_Y represent the inertia of straight and the rotational motion, respectively. B_S and B_Y represent the viscous of each motion. τ_S and τ_Y stand for the straight and yaw torque, respectively. d_S and d_Y are the disturbance of the straight and yaw motion.

2.3 Conclusion of this Chapter

Using this modeling method, the motion of PAW can be divided into two parts – the common component and the differential component. It can be seen from the equation 2-9 and 2-10 that the straight and rotational potions of PAW are proportional to the common component and the differential component, respectively.

Since users will feel different in the lateral and longitudinal directions, using this modeling method, the control system can be designed independently for lateral and longitudinal directions.

Similar modeling methods can also be found in [16] and [19].

Chapter 3

Design of Force Sensorless Power Assist Control System and Experimental Setup

In chapter two, the modeling of PAW considering the lateral and longitude directions is introduced.

In this chapter, the design method for force sensorless power assist control (FSPAC) system will first be introduced, then the experimental devices and environments will be introduced.

3.1 Human Force Detection

In this section, a disturbance observer (DOB) based force estimator is applied to detect external force. The external force includes human force and the disturbance. After getting external force from DOB based force estimator, human force separation algorithms are used to get human force.

3.1.1 Low acceleration estimator based disturbance observer

A low acceleration estimator based force disturbance observe shown in Figure 7 is used to detect external force. It is obviously that wheelchairs often move in a low speed and low acceleration which makes it more difficult to get high-accurate acceleration information from the encoders. To get high accurate acceleration, it is common to use a high resolution encoder. However, to use a high resolution encoder may make the entire system expensive. If the low-resolution encoders can be used in the application, the cost can be cut down. The low-acceleration estimator (LAE) [20] developed by Lee *et al.* is employed to provide the required

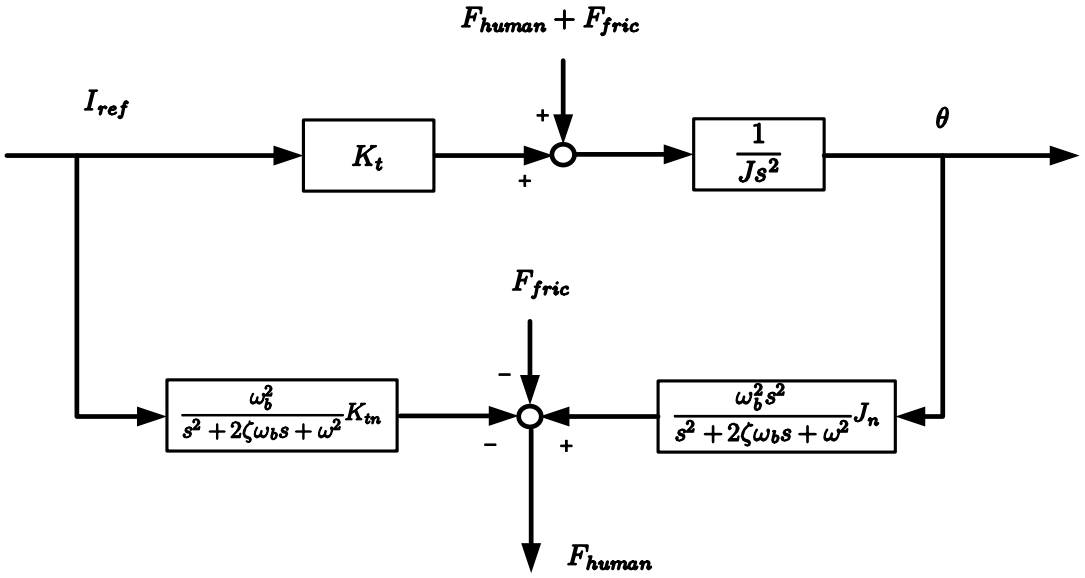

Figure 7: The low-acceleration estimator based torque observer

acceleration and velocity. The external force F_{ext} can be estimated as

$$F_{ext} = \frac{\omega_b^2(s^2 J_n\theta - I_{ref}K_{tn})}{s^2 + 2\zeta\omega_b s + \omega_b^2}\frac{1}{R} \tag{3-1}$$

In real experiments, ω_b is set as 10 rad/s to take balance between the tracking capability and the estimator performance. ζ is set as 0.707 to provide the fast response without overshot.

3.1.2 Human force extraction

The external force can be detected by a DOB based force estimator. However, the friction force are also included in the external force. As a human-machine system, it is important for PAW to sense the human force, and the assist torque should be just applied to human force. That means it is important to separate human force from the entire external force. In this paper, two methods are developed to separate human force from the external force. The first method as shown in Figure 8(a) is to model the disturbance as accurate as possible, the human force can be obtained by subtracting disturbance from the external force. The second method shown in Figure 8(b) is to estimate human force and the disturbance simultaneously using the different characters of human force and the disturbance force. This two method will be discussed in Chapter four, five and six.

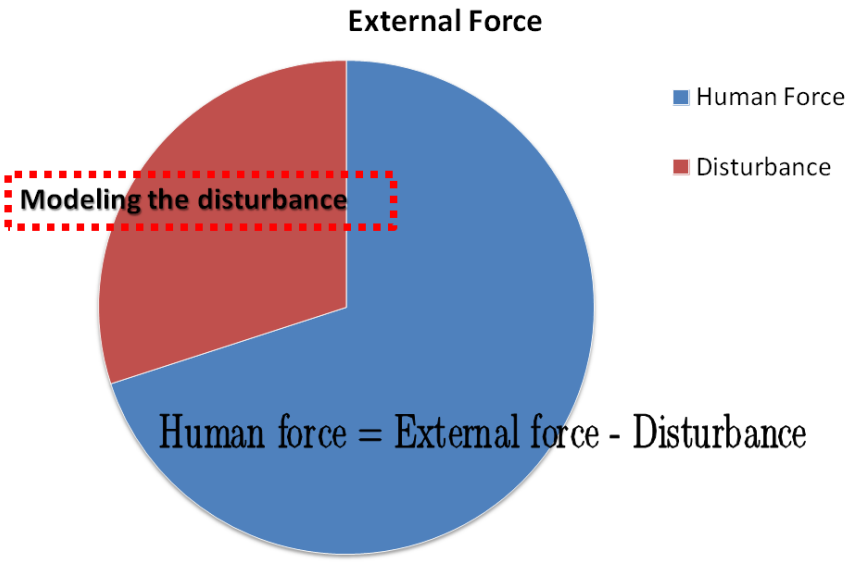

(a) Modeling the disturbance.

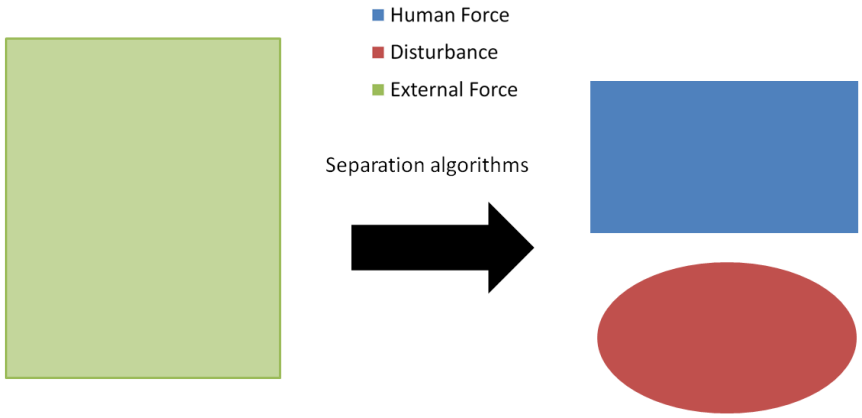

(b) Using different characteristics.

Figure 8: Two methods to separate human force

3.2 Power Assist Control

Power assist control is applied to the estimated human force. The human force will be amplified by multiplying the assistance gain. As is introduced in Chapter 2, PAW can be modeling by considering longitudinal and the lateral directions. Therefore, the assistance gains can be designed for longitudinal and the lateral directions independently [8]. The assistance gain can also be adjusted according to the real environments.

It should also be noticed that the nominal model can not always be correct, if the input is continuous, the wheelchair may keep accelerating. An impedance is needed here to avoid this effect. Then the velocity reference ω_{ref} can be generated.

3.3 Overall Control System

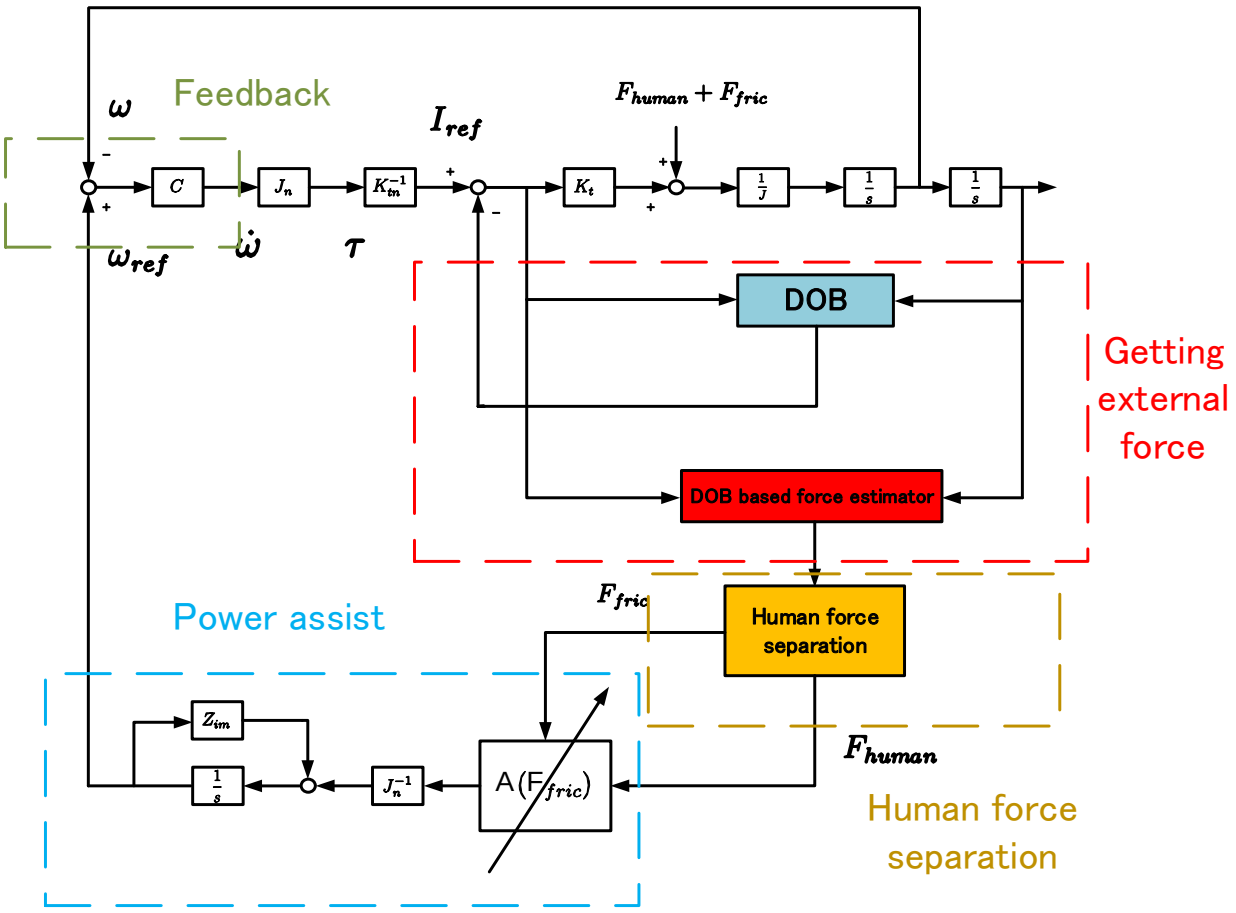

Figure 9: The entire control system

Figure 9 shows the overall control system. Subscripts $human$, $fric$, n and ref stand for input from the human, input from friction force, nominal value and reference, respectively.

The control system can be divided into four parts. The first part is a DOB and a DOB based force estimator. A DOB is constructed here for the system to track for the reference. The robustness of the whole system is improved by using the DOB. The DOB based force estimator is used in the system to estimate external force including human force and friction force. The second part aims to separate human force and the disturbance to ensure the assist force will only be applied to the human force. The third part is the power assist part, the power assist gain can be designed according to the estimated friction force coefficient, if the friction force coefficient is high, the assist gain can also be set high to support the user. If the environment changes, the friction force can be estimated again by resetting the program. Finally, the velocity reference will be tracked in the feedback loop.

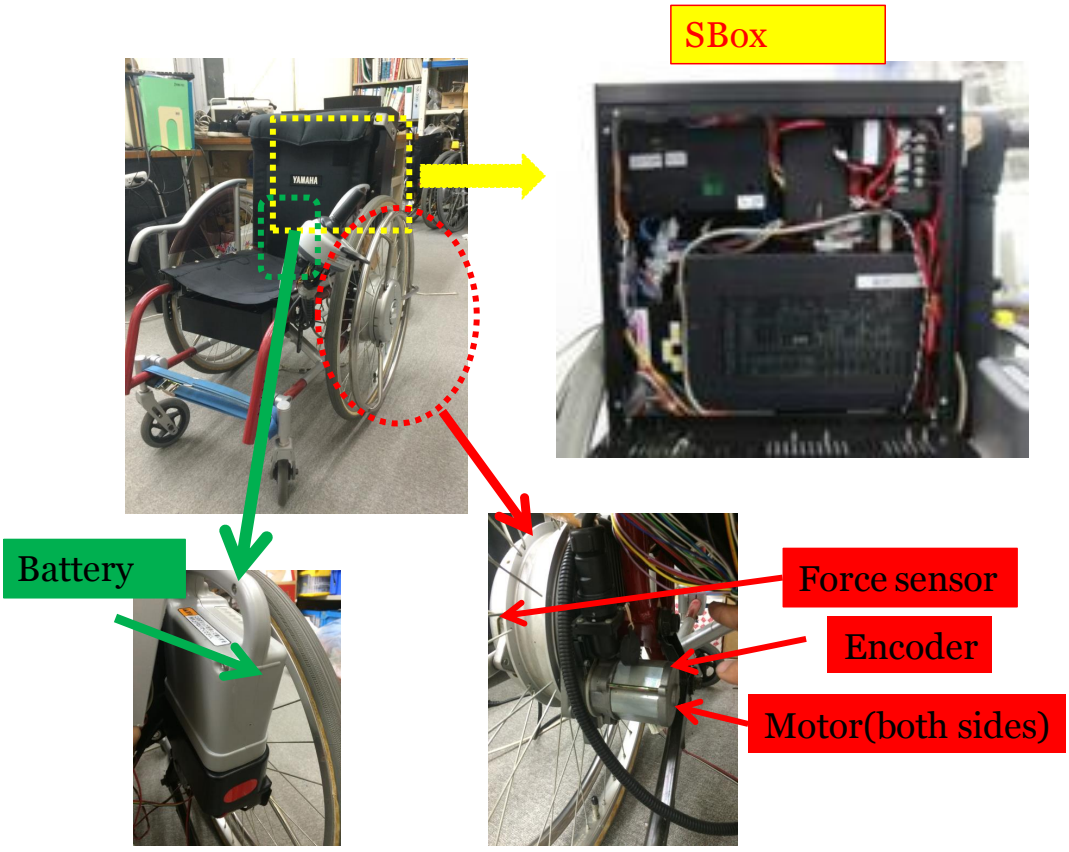

Figure 10: Experimental setup

3.4 Experimental setup

In this section, the experimental devices will be introduced.

The experimental set up is shown in Figure 10. The wheelchair used here is JW-II which is produced by YAMAHA. Force sensors are set in handrims so the users can move the wheelchair by propelling the hand-rims. It should be noticed that the measured data from force sensors here is only used to evaluate the proposed method for human force estimation. And the force sensors will not be used in the control system. The velocity information can be obtained from the encoders. More information is shown in Table 2. The parameters used in the experiments are shown in Table 3.

3.5 Conclusion

In this chapter, the entire FSPAC system for PAW the experimental devices are introduced. The entire control system can be divided into four parts: a DOB and a DOB based force estimator to estimate external force, an algorithm to obtain human force from external force,

Table 2: Variables of equipments

Parts	Type	Company
PAW	JW-II	YAMAHA
DSP	s-BOX	MTT
Encoder	RE20F-100-200	COPAL ELECTRONICS

Table 3: Parameters of the human-PAW system

Mass of the wheelchair and human	M	105 kg
Radius of the wheel	R	0.33 m
Inertia of the straight motion (Lab)	J_s	5.73 kgm^2
Inertia of the yaw motion (Lab)	J_Y	7.19 kgm^2

the power assist part to generate velocity reference. A feedback loop to tract the velocity reference.

In Chapter four, five and six, the methods to extract human force (human input timing) will be discussed.

Chapter 4

Force Sensorless Power Assist Control for Wheelchairs Considering Caster Effects

In this chapter, the caster effects are considered into the entire system.

A Disturbance Observer (DOB) based force estimator is applied to PAW to estimate external force. However, the external force includes the human force, the rolling resistance and the sliding resistance.

The rolling resistance can be compensated using the Viscous and Coulomb friction model easily.

When the directions of PAW is changed, a caster orientation observer is applied to detect the movement of the casters firstly, aiming to reduce the influence on the entire system by the sliding force. Then the sliding resistance is compensated. By compensating rolling resistance and sliding resistance, the human force can be estimated correctly during both straight forward and turning around.

Simulation and experimental results demonstrate the validity of the proposed method.

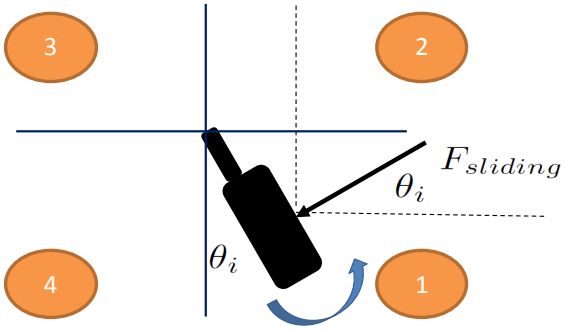

Figure 11: The configuration of a caster

4.1 Resistance

Basically speaking, there are two kinds of resistance for PAW — the rolling resistance and the sliding resistance.

4.1.1 Rolling resistance

The Coulomb and Viscous friction model is usually used to compensate for the rolling resistance in the right and left sides, respectively. Considering the safety, the power-assist control is set to start when $v>0$. The Coulomb coefficients and Viscous coefficients of each side are shown in Table 4.

Table 4: Parameters of the friction coefficients

Viscous coefficient	0.25 Nm/(rad/s)
Coulomb coefficient	3 Nm

4.1.2 Sliding resistance

When the wheelchair is turning around, the sliding force from the casters will have a high influence on the entire system[21][22]. Assuming each caster have a rigid body with sliding resistance acting on it. This configuration is illustrated in Figure 11.

The sliding resistance can be written as equation 4-1 and 4-2. Where C is a constant value which is proportional to the coefficient of sliding force and the weight supported by the caster. If the position of the caster and the angular velocity of the caster is known, the sliding resistance

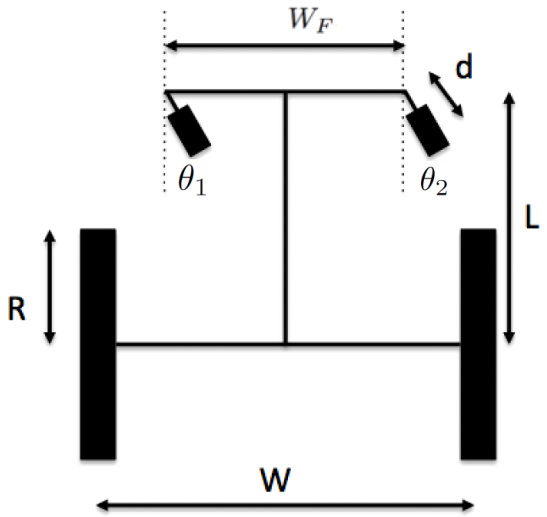

Figure 12: Vertical view of a wheelchair

can be compensated.

$$\tau_s = C\text{sgn}(\dot{\hat{\theta}}_{\text{i}})\sin(\hat{\theta}_{\text{i}})(\text{Phase 1 and 2}) \text{ or } -C\text{sgn}(\dot{\hat{\theta}}_{\text{i}})\sin(\hat{\theta}_{\text{i}})(\text{Phase 3 and 4}) \tag{4-1}$$

$$\tau_y = C\text{sgn}(\dot{\hat{\theta}}_{\text{i}})\cos(\hat{\theta}_{\text{i}})(\text{Phase 1 and 4}) \text{ or } -C\text{sgn}(\dot{\hat{\theta}}_{\text{i}})\cos(\hat{\theta}_{\text{i}})(\text{Phase 2 and 3}) \tag{4-2}$$

Therefore, the human torque can not be detected correctly when turning around if we only consider about the rolling resistance. Since it is difficult to know the position and the angular velocity of each caster directly. A caster orientation observer [23] is used here to solve the problem.

4.2 Caster Orientation Observer

The vertical view of the wheelchair will be shown in Figure 12. The parameters of the wheelchair are shown in Table 5. It is difficult to measure the angular and the velocity of the angular directly. Even some sensors can be set up in the system, it will increase the cost of the whole system. A method to estimate the orientation of the wheelchair's caster wheels is proposed in [23]. It is shown that the angular and the angular velocity of the casters can be written as

$$\dot{\hat{\theta}}_1 = \frac{2R\omega_Y}{dW}(L\cos\hat{\theta}_1 + \frac{W_F\sin\hat{\theta}_1}{2} - d) - \frac{R\omega_s}{d}\sin\hat{\theta}_1 \tag{4-3}$$

$$\dot{\hat{\theta}}_2 = \frac{2R\omega_Y}{dW}(L\cos\hat{\theta}_2 - \frac{W_F\sin\hat{\theta}_2}{2} - d) - \frac{R\omega_s}{d}\sin\hat{\theta}_2 \tag{4-4}$$

It should be noted that a sudden change in the wheelchair direction will causes a brief instability. But, in real environment, the direction of the wheelchair will not always change,

Table 5: Parameters of the wheelchair

R	0.3 m
W	0.6 m
W_F	0.47 m
L	0.4 m
d	0.07 m

the error can be assumed to be small, and this instability will not amplify the error enough to affect whole estimate.

Figure 13 shows the simulation results for this caster orientation observer. From the simulation results we can know that the orientation and the orientation rate of each caster can be estimated just using the straight and the yaw velocity of the wheelchair. The velocity information can be got from the encoders. It dosen't need any other sensor to estimate the states of both casters.

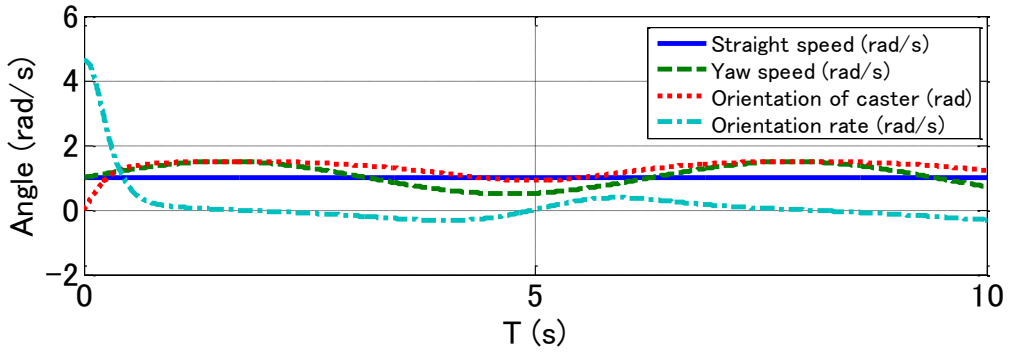

(a) Left caster.

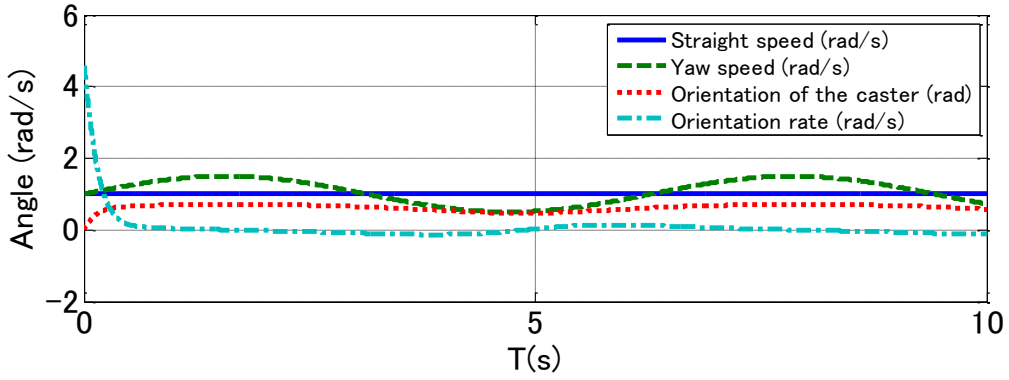

(b) Right caster.

Figure 13: The simulation results for cater orientation observer

4.3 The Convergence of the Caster Orientation Observer

Essentially, the caster orientation observer is an open loop observer, therefore, it is important to ensure that the estimated angle will converge to the real value. The stability will be proven in the following part. Since the two casters are symmetrical and independent, the analysis method of the two casters will be same, in this paper, the observer for θ_1 will be taken as an example.

First, the estimation error is defined as $\tilde{\theta}_1$ which can be expressed as the difference between the estimated value $\hat{\theta}_1$ and the real value θ_1.

$\tilde{\theta}_1$ should converge to 0 to guarantee the stability of the entire observer. The condition for this convergence can be obtained by discussing the local stability using the linearization of $\dot{\hat{\theta}}_1$ around the real value θ_1[24].

Define

$$f(\hat{\theta}_1) \simeq f(\theta_1) + \frac{df(\hat{\theta}_1)}{d\hat{\theta}_1}|_{\hat{\theta}_1=\theta_1}(\hat{\theta}_1 - \theta_1). \tag{4-5}$$

For $f(\hat{\theta}_1)$=$\dot{\hat{\theta}}_1$

$$(\dot{\hat{\theta}}_1 - \dot{\theta}_1) \simeq \frac{d(\dot{\hat{\theta}}_1)}{d\hat{\theta}_1}|_{\hat{\theta}_1=\theta_1}. \tag{4-6}$$

where $d(\dot{\hat{\theta}}_1)/d\hat{\theta}_1$ can be obtained using the equation 4-3. Then, using $\tilde{\theta}_1$ and $\dot{\tilde{\theta}}_1$ to replace $(\hat{\theta}_1 - \theta_1)$ and $(\dot{\hat{\theta}}_1 - \dot{\theta}_1)$, the linear approximation of error dynamics can be expressed as

$$\dot{\tilde{\theta}}_1 \simeq -\left(\frac{2R\omega_Y}{dW}(L\sin\theta_1 - \frac{W_F\cos\theta_1}{2}) + \frac{R\omega_s}{d}\cos\theta_1\right)\tilde{\theta}_1. \tag{4-7}$$

Let

$$\bigsqcup_1 = \frac{2R\omega_Y}{W}(L\sin\theta_1 - \frac{W_F\cos\theta_1}{2}) + R\omega_s\cos\theta_1 \tag{4-8}$$

The error dynamics can be expressed as

$$\dot{\tilde{\theta}}_1 \simeq -\frac{\bigsqcup_1 \tilde{\theta}_1}{d} \tag{4-9}$$

The similar equation can also be obtained following the same approach, the caster i yields

$$\dot{\tilde{\theta}}_1 \simeq -\frac{\bigsqcup_i \tilde{\theta}_i}{d} \tag{4-10}$$

It is known that the solution of equation 4-10 will converge to zero as time $t \to \infty$ only if $\bigsqcup_1$ is always bigger than zero. It can be known from this conclusion that when the caster is rolling forward the stability of the estimator can be ensured.

Similarly, the stability of the caster orientation estimator can be also evaluated with a linearization around $\theta_1 + 2k\pi$ for $k \in Z$, the error dynamics can be written as

$$\dot{\tilde{\theta}}_1 \simeq -\frac{\bigsqcup_i(\tilde{\theta}_i - 2k\pi)}{d} \tag{4-11}$$

Equation 4-11 means when the caster is moving forward, the estimation error will converge to $2k\pi$ depending on the initial condition.

A linearization around $\theta_1 + (2k+1)\pi$, the error dynamics is

$$\dot{\tilde{\theta}}_1 \simeq \frac{\bigsqcup_i(\tilde{\theta}_i - (2k+1)\pi)}{d} \tag{4-12}$$

This means the estimation error will converge to π when the caster is rolling backwards. However, there is a condition that the caster wheel must be propelled in an unstable way. This will not be a problem since the human input can not always be the same. But a deviate will happen as is shown in Figure 14, In this chapter, we assume that the deviate will not last for a long time so the effect will not have a deep effect on the entire estimation.

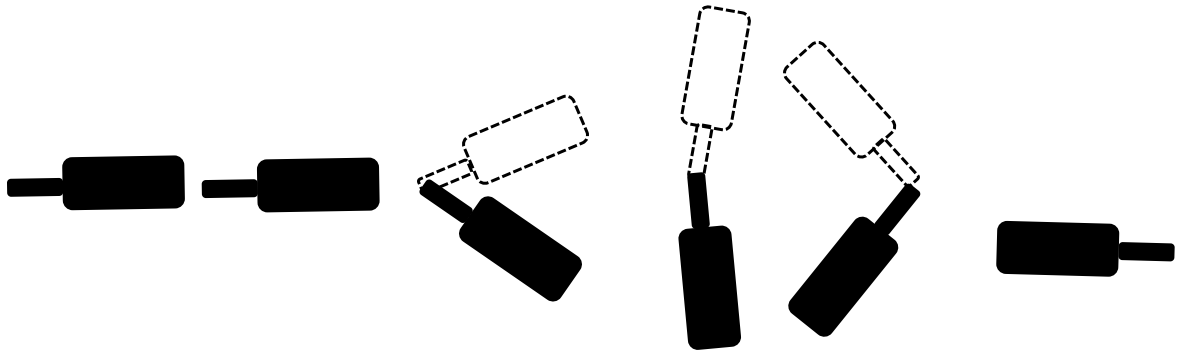

Figure 14: Illustration of the deviate

4.4 Experimental Condition

4.4.1 Experiment 1: Going straight

Figure 15(a) shows experimental environment of Experiment 1. The users will move the wheelchair going straight forward and then going straight backward. The angular of both casters will change 180 degrees when the direction of the wheelchair is changing. The purpose of this experiment is to verify the effect of sliding resistance when the directions of both casters change suddenly.

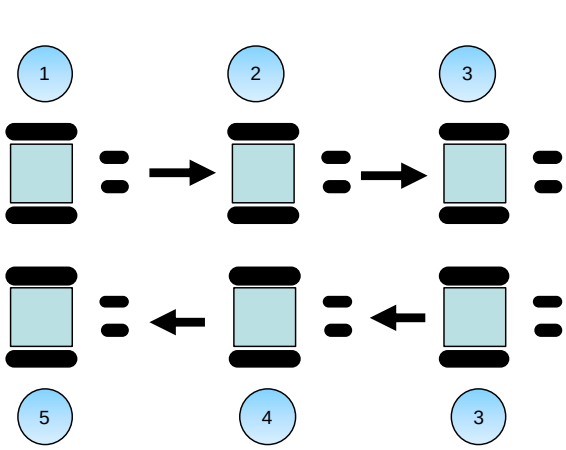

(a) Experiment 1.

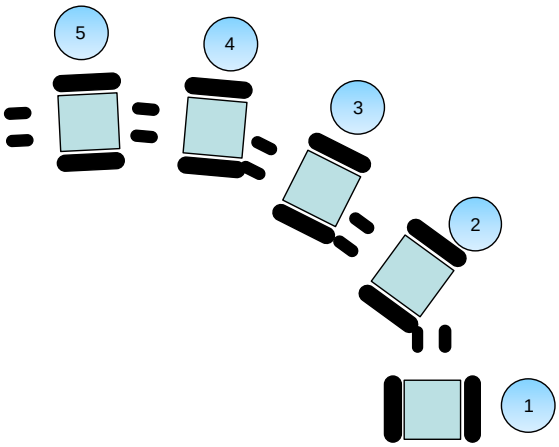

(b) Experiment 2.

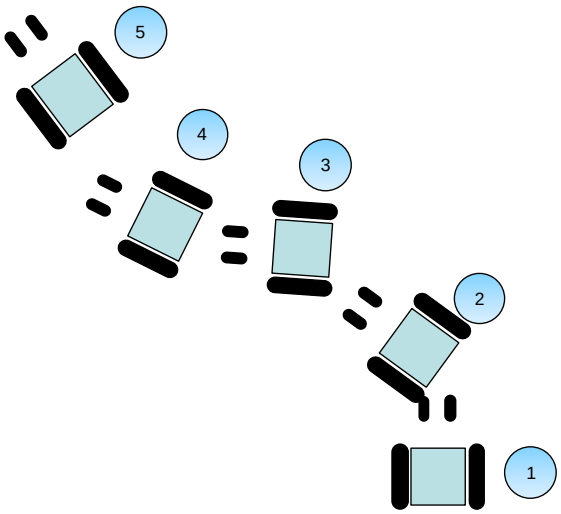

(c) Experiment 3.

Figure 15: Experimental conditions

4.4.2 Experiment 2: Going straight with turning left

Figure 15(b) shows experimental environment of Experiment 2. In Experiment 2, the directions of the casters will change smoothly. We will verify that the sliding resistance compensation is important in this case.

4.4.3 Experiment 3: Going straight with sinusoidal turning

Figure 15(c) shows experimental environment of Experiment 3. The direction of casters will change a lot. The compensation for sliding resistance is extremely important in this case.

4.5 Experimental Results

4.5.1 Experiment 1: Going straight

Experimental results of going straight are shown in Figure 16. The above part of Figure 16 shows the torque information when going straight. The red line is the real human torque which is detected by the torque sensor. The green dot line stands for the estimated human torque with previous method which only consider about the rolling resistance. The blue line represents the estimated human torque by the proposed method which consider about both the rolling resistance and the sliding resistance.

From 12.5 seconds, the user start to move the wheelchair backward. The human torque changed its direction. And from Figure 16, the angular of the casters changed π. In this experiment, the wheelchair move straight most of the time, so the sliding resistance will not have a obvious effect on the estimated human force. However, when the wheelchair start to change its direction, the proposed method shows a better performance.

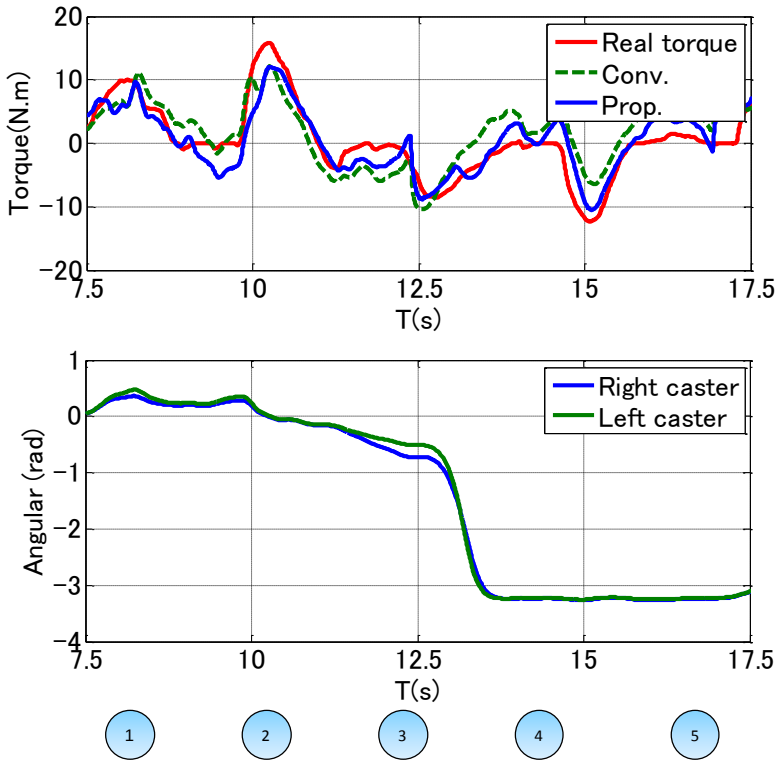

Figure 16: Going straight (Experiment 1)

4.5.2 Experiment 2: Going straight with turning left

Experimental results of going straight with turning left are shown in Figure 17.

The above part of Figure 17 shows the torque information when going straight with turning left. The color code of each line is same as that of Figure 16.

The under part of Figure 17 shows the change of the angular of the casters. The angular will change a lot between the whole movement.

In this experiment, as shown in Fig.15(b). The wheelchair will go straight with turning left. The angular of caster will change a lot during 7 to 15 seconds. In this case, the sliding resistance will have a large effect on the human force estimation.

The results of the proposed method are much better than the previous one. As is shown in Figure 17, when the caster changed its position, the previous method can not estimate the human force accurately, especially between 12 to 14 seconds. However, by using the proposed method, the estimated human torque is much better than the previous one.

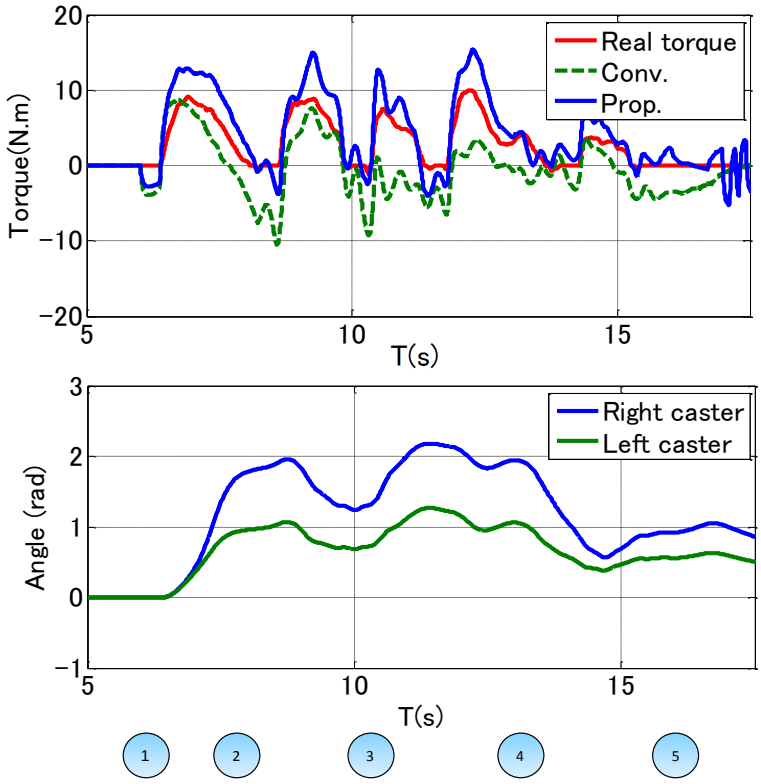

Figure 17: Going straight with turning left (Experiment 2)

4.5.3 Experiment 3: Going straight with sinusoidal turning

Experimental results of going straight with sinusoidal turning are shown in Figure 18.

The above part of Figure 18 shows the torque information when going straight with sinusoidal turning. The color code of each line is same as that of Figure 16.

The under part of Figure 18 shows the change of the angular of the casters. The angular will change a lot between 7.5 to 9 seconds, and 13 to 15 seconds.

Since the angular of the caster changed a lot between 7.5 to 9 seconds, and 13 to 15 seconds, the estimated human force should be effected by the sliding resistance among this moment. Actually, as shown in Figure 18, the experimental results exactly show this phenomenon. So, the proposed method is also effective in this case.

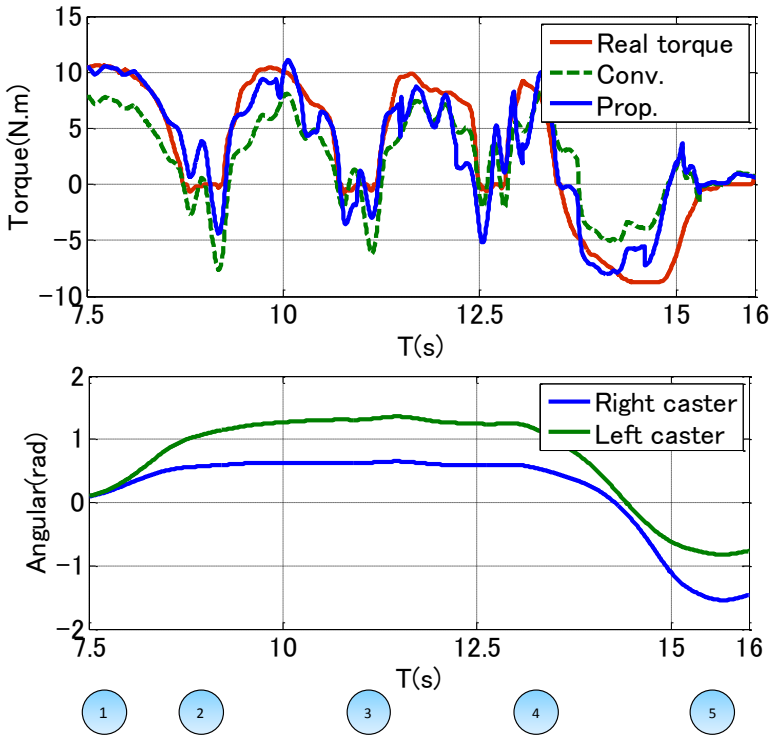

Figure 18: Going straight with sinusoidal turning (Experiment 3)

4.6 Conclusion

4.6.1 About the experimental results

By considering the sliding resistance, the proposed method shows its superiority compared with the previous one. From the experimental results, it is obvious that the sliding force may have a bad effect on human force estimation especially when the angular of the caster changed a lot. But by compensating the sliding resistance, the human torque can be estimated accurately.

4.6.2 About the proposed method

By compensating the sliding resistance, the results get better. However, we also need to know the sliding coefficients of the environment. This makes the proposed method complicated.

4.6.3 About caster orientation observer

The only information needed for this observer is the straight and yaw angular velocity which can be obtained by encoders. If the orientation of casters changed suddenly and largely, this observer may not work correctly. But it is only temporarily, the caster will eventually change its orientation and make estimator stable again.

4.6.4 About the future work

In this chapter, a method by compensating rolling resistance and sliding resistance is proposed. By using the proposed method, the human torque can be estimated more correctly than previous methods especially when the wheelchair is changing the direction. But, this method is more complicated than the previous one. A statistical method can be used to separate human force from the external forces will be introduced in Chapter Five. And no compensation will be needed.

Chapter 5

Force Sensorless Power Assist Control for Wheelchair on Flat Road Using Recursive Least Square with Multiple Forgetting

In chapter four, human force is obtained by compensating the the rolling friction and the sliding friction. However the resistance is difficult to modeled. When the environment changes, the coefficients need to be modeled again. This make the force sensorless control difficult to be realized. In the conventional method, the friction force is compensated using the Viscous and Coulomb friction model. In this chapter, a Recursive least square (RLS) with multiple forgetting method is used to separate human force and the friction force. By using this method, it will not be necessary to model friction force beforehand. Furthermore, the friction coefficient can also be estimated by using this method, therefore, the assist rate can be adjusted in different environments. Simulation and experimental results demonstrate the validity of the proposed method.

5.1 Separating Human Force and Friction Force

The external force can be obtained by using a DOB based force estimator which includes human force and friction force. In conventional methods, the friction force should be compensated using a friction model such as the Viscous and Coulomb friction model. It is inconvenient since the viscous and the coulomb coefficients need to be identified beforehand. Noticing that the friction force can be regarded as a constant value [21], we can simplify this problem as below

$$F_{ext} = F_{human} - \mu M g \tag{5-1}$$

Where F_{ext} means the external force including human force and friction force. F_{human} is the human force. μ is the friction coefficient, M is the mass of the overall system, and g is the gravitational acceleration. F_{human} is time varying and the parameter μ is a constant value. If we differentiate the equation 5-1, the constant part (friction part) will be disappeared. However, by using this method to calculate human force, the drift will happen since it needs to integrate the differential part. In this paper, the Multiple forgetting Recursive Least Square method is used here to estimate the human force and the friction coefficient.

5.2 Multiple Forgetting RLS Method

5.2.1 The multiple forgetting RLS algorithm

In [25], a multiple forgetting RLS method is proposed to estimate two parameters when one parameter is constant and another is time-varying. In the application for force sensorless power assist control for PAW, this method is used to estimate human force and friction coefficient simultaneously. We can conclude this problem in the following structure:

$$F_{ext} = F_{human} - \mu M g, \tag{5-2}$$

$$y = \phi^T \theta, \phi = [\phi_1, \phi_2]^T, \tag{5-3}$$

$$\theta = [\theta_1, \theta_2]^T = [F_{human}, \mu]^T, \tag{5-4}$$

$$y = F_{ext}, \phi = [\phi_1, \phi_2] = [1, -Mg]. \tag{5-5}$$

The algorithm to separate human force and the friction coefficient can be written as follow:

$$\hat{\theta}(k) = \hat{\theta}(k-1) + K(k)(y(k) - \phi^T(k)\hat{\theta}(k-1)) \tag{5-6}$$

$$K(k) = \frac{1}{1+\frac{P_1(k-1)\phi_1(k-1)^2}{\lambda_1}+\frac{P_2(k-1)\phi_2(k-1)^2}{\lambda_2}} \begin{bmatrix} \frac{P_1(k-1)\phi_1(k)}{\lambda_1} \\ \frac{P_2(k-1)\phi_2(k)}{\lambda_2} \end{bmatrix} \tag{5-7}$$

$$K_1(k) = P_1(k-1)\phi_1(k)(\lambda_1 + \phi_1^T(k)P_1(k-1)\phi_1(k))^{-1} \tag{5-8}$$

$$P_1(k) = (I - K_1(k)\phi_1^T)P_1(k-1)\frac{1}{\lambda_1} \tag{5-9}$$

$$K_2(k) = P_2(k-1)\phi_2(k)(\lambda_2 + \phi_2^T(k)P_2(k-1)\phi_2(k))^{-1} \tag{5-10}$$

$$P_2(k) = (I - K_2(k)\phi_2^T)P_2(k-1)\frac{1}{\lambda_2} \tag{5-11}$$

5.2.2 The simulation results to separate human torque

The simulation results are shown in Figure 19 ,20 and 21. In this simulation, human force is expressed in a sine function, and the friction coefficient is set as 0.012. The mass of the entire system is set as 100 kg. g is set as 9.8 m/s^2. The external force obtained from DOB is expressed in Figure 19, the friction force is assumed to be a constant value. We assume that the environment will not change, so the forgetting factor λ_2 represents the changing rate of the friction coefficient will be set as 1. The forgetting λ_1 for human force is set as 0.95 according to the force characteristic. According to the simulation results, it is clear that by using this method, the human force can be correctly separated from the external force without friction compensation beforehand.

5.2.3 Discussion about RLS with multiple forgetting

The normal type of RLS with multiple forgetting[26] can be written as

$$\hat{\theta}(k) = \hat{\theta}(k-1) + K^{'}(k)(y(k) - \phi^T(k)\hat{\theta}(k-1)) \tag{5-12}$$

$$K^{'}(k) = P(k-1)\phi(k)(1 + \phi^T(k)P(k-1)\phi(k))^{-1} \tag{5-13}$$

$$P(k) = \Lambda^{-1}(I - K^{'}(k)\phi^T(k))P(k-1)\Lambda^{-1} \tag{5-14}$$

$$\Lambda = diag\{\lambda_1, \lambda_2\} \tag{5-15}$$

The simulation results to separate human force and the friction coefficient are shown in Figure 22, 23 and 24. In this method, λ_1 for human force is set as 0.7 to ensure the good tracking performance.

The method proposed in [25] and [26] have some difference. Firstly, Equation 5-6 is similar to the standard update form of the well known RLS estimation with with multiple forgetting (Equation 5-12)[26]. However, the gains are different. The covariance of RLS with Multiple forgetting proposed in [25] is diagonal, while the normal one has a crossterm of $P_{12}(k-1)$ and

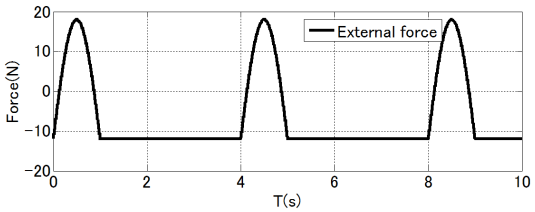

Figure 19: External force from DOB

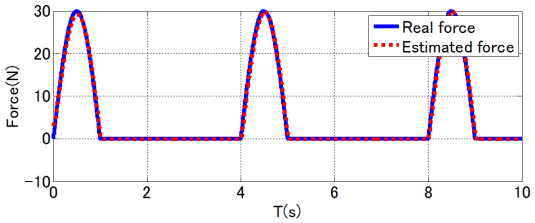

Figure 20: Human force

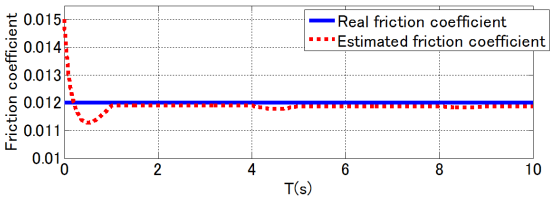

Figure 21: Friction coefficient

$P_{21}(k-1)$. This can reduce the calculation. And the algorithm proposed by [26] is stronger with noise. The simulation about their characteristics toward same noise is shown in Figure 25. For this application, both algorithms are alright because there is a low pass filter in the DOB and the DOB based force estimator part, the effect from the noise will not have a large effect toward the overall system.

In this paper, the first algorithm is used to separate human force and the friction force.

5.3 Experiment

5.3.1 Experiment 1: Going straight

Figure 26(a) shows the experimental environment of Experiment 1. The users will move the wheelchair going straight forward and then going straight backward. The purpose of this experiment is to verify the effectiveness of the proposed human force estimation method when going straight.

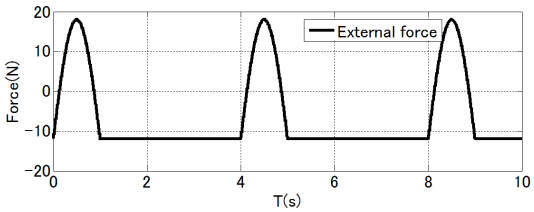

Figure 22: External force from DOB

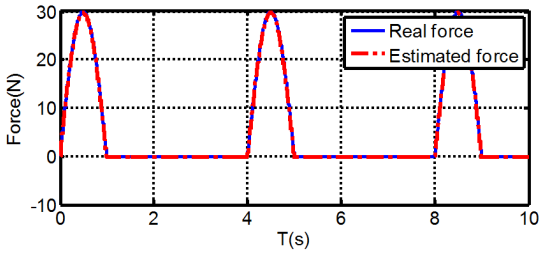

Figure 23: Human force

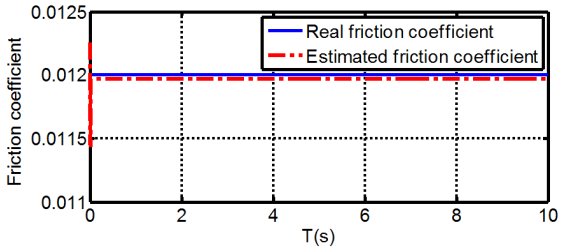

Figure 24: Friction coefficient

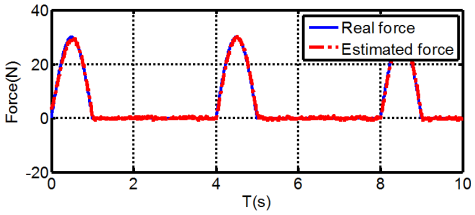

(a) Human Force with noise, Multiple forgetting RLS [25].

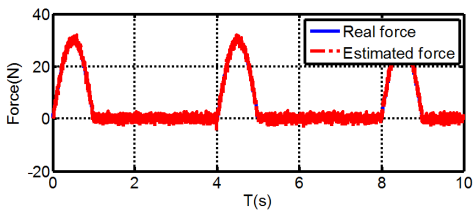

(b) Human Force with noise, Multiple forgetting RLS [26].

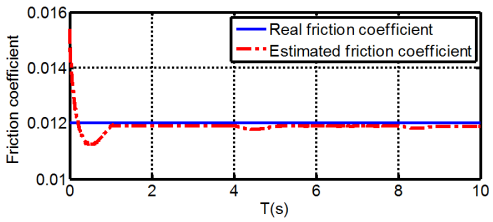

(c) Friction coefficient with noise, Multiple forgetting RLS [25].

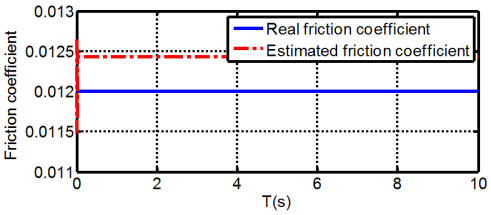

(d) Human Force with noise, Multiple forgetting RLS [26].

Figure 25: The characteristics toward noise

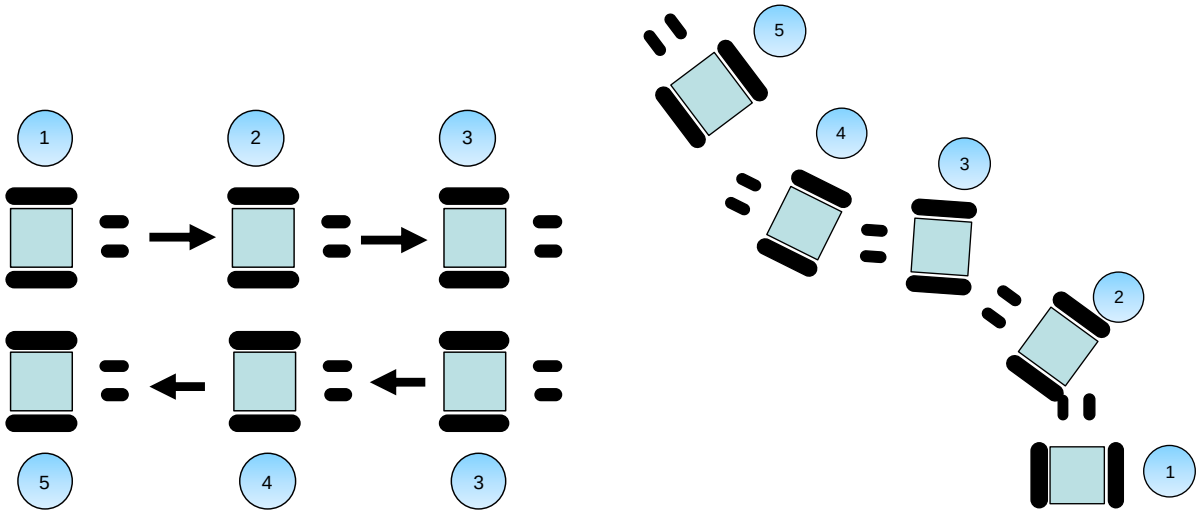

(a) Experiment 1: Going straight.

(b) Experiment 2: Going straight with sinusoidal turning.

Figure 26: Experimental condition

5.3.2 Experiment 2: Going straight with sinusoidal turning

Figure 26(b) shows experimental environment of Experiment 2. The wheelchair will move with sinusoidal turning. We want to verify the effectiveness of the proposed method when wheelchair is turning.

5.4 Experimental Results

5.4.1 Experiment 1: Going straight

Experimental results of going straight are shown in Figure 27. The blue line is the real human torque which is detected by the torque sensor. The green dashed line stands for the estimated human force with conventional method compensating the friction force by using the Viscous and Coulomb friction model. The red dot line represents the estimated human force by the proposed method using RLS with multiple forgetting.

The user will drive the wheelchair move forward until 12.5 seconds. From 12.5 seconds, the user started to move the wheelchair backward. The proposed method show good performance even there is no friction force compensation beforehand.

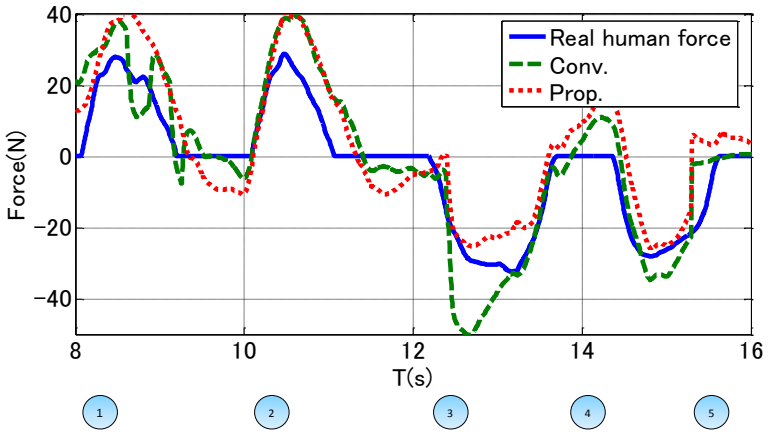

Figure 27: Experiment 1: Going straight

5.4.2 Experiment 2: Going straight with sinusoidal turning

Experimental results of going straight with sinusoidal turning are shown in Figure 28. Figure 28 shows the force information when going straight with sinusoidal turning. The color code of each line is same as that of Figure 27.

In this experiment, as shown in Figure 26(b), the wheelchair will go straight with sinusoidal turning. The user is changing the direction between 7.5 to 9 seconds, and 13 to 15 seconds, the human force can not be estimated as well as the Experimental 1. That is because when the direction of wheelchair is changing, there will be some other disturbance from the casters or axle[21][22]. But in general, the proposed method performs well.

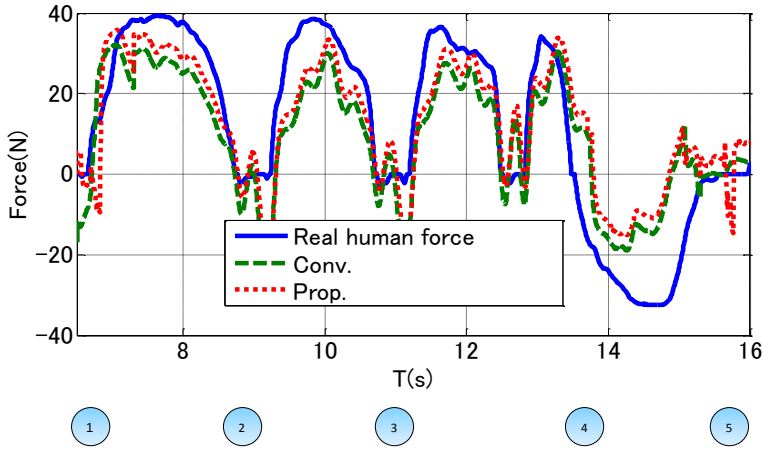

Figure 28: Experiment 2: Going straight with sinusoidal turning

5.5 Conclusion

5.5.1 About RLS with multiple forgetting

There are two algorithms, both are alright for this application. In this application, different forgetting factors can be set for human force and the friction coefficient by assuming the friction coefficient will not change in a certain environment. Notice that this method is applied for the PAW for the user type, the human input change much faster than the friction force. For the caregiver type, more discussion is needed.

5.5.2 About the experimental results

Using RLS with multiple forgetting, no friction force compensation will be needed beforehand and the estimated results turn out to be good. The proposed method can also be applied to various environments with only resetting the program.

5.5.3 About the future work

In this chapter, a method using RLS with multiple forgetting to separate human force and friction force is proposed in this paper. By using the proposed method, the human force can be estimated without compensating the friction force. However this method can not be used to separate the changing disturbance. In Chapter six, a new method is developed to estimate human input timing in various environments.

Chapter 6

Human Input Timing Estimation using Different Changing Rates of Human Force and Disturbance

In this chapter, a method using different changing rate of human force and disturbance will be introduced to estimate human input timing. In chapter four and five, two methods are proposed to obtain human force in the flat road environment. However, if the disturbance is changing, this two methods can not be used. In this chapter, a method considering the different changing rates is developed to estimate the human input timing. Using this method, the assist force can be given when the people is propelling the handrims. This method can be used in both flat road and the slope road environments, no compensation beforehand will be needed.

6.1 The Characteristic of Human Force and Disturbance

According to [17][18], as is shown in Figure 29, the frequency of input force when users are driving wheelchairs is always between 0.5Hz to 1.5Hz. An assumption is set here–the disturbance from friction force and the gravity force change much slower than human input force. Therefore, by judging the different change rates, it is possible to estimate the timing of human input.

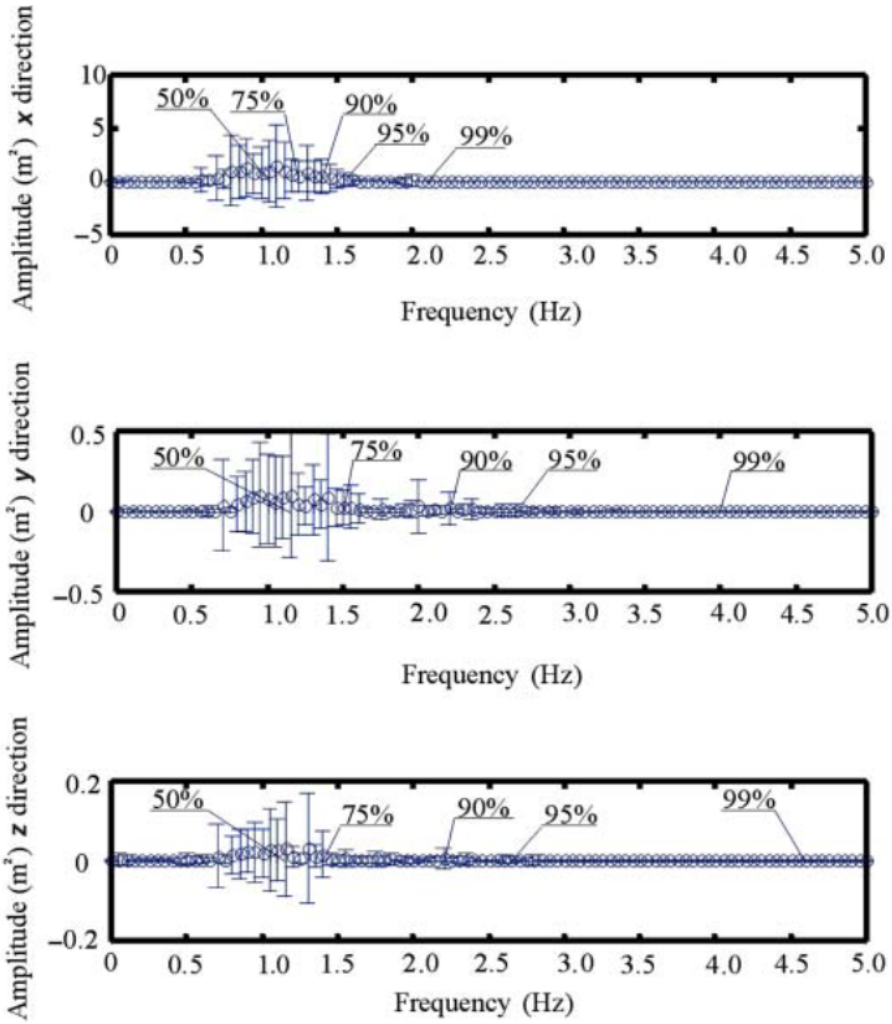

Figure 29: Propulsion frequency characteristics[17]

6.2 Human Input Timing Estimation using Different Changing Rates of Human Force and Disturbance

It can be assumed that the changing rate of human input is much faster. If the system can know the timing when human give the input, many assist algorithms can be designed.

It is easy to consider using the differential value to describe the changing rate. However, it is difficult to judge the changing rate if only one set of data is considered. So, some statistical processing is needed. In the real system, the sampling frequency is 1kHz. Here, data in 0.1s are used to judge whether the human is given force to the handrim. Since data near the present time show more representative for the present situation, therefore, weighting factors are used to represent the effectiveness of the data.

The proposed method can be written as shown in the equation 6-1 and 6-2. ω_i stands for weighting factor for changing of the external force on the moment i, F_i represents the external force on moment i and Equation 6-2 is an arithmetic sequence.

$$F_w = \omega_m(F_i - F_{i-k}) + \omega_{m-1}(F_{i-1} - F_{i-k-1}) + ... + \omega_1(F_{i-m} - F_{i-k-m}) \tag{6-1}$$

$$\omega_m + \omega_{m-1} + ... + \omega_1 = 1 \tag{6-2}$$

By setting a proper threshold, the simulation result is show in Figure 30(a). In this simulation, k equals to 80, ω_1 is 0.01 and m equals to 20. The threshold is set as 0.15. If F_w is bigger than the threshold, that means there exists human input. The blue line stands for the external force obtained by DOB based estimator. The green line represents the human force, and the red line is the order for judgment. If human input exists, the value of the red line should be 10. If human input doesn't exist, the red line should be 0.

In Figure 30(a), the threshold is set as 0.15. There is still some parts in the peak portion which can not be judged. Finding that these parts will last less than 0.1 seconds, adding another rule that when the order changes, it must last longer than 0.1 seconds. The improved simulation result is shown in Figure 30(b).

It will cause some delay (less than 0.1s) by using this method to estimate the human input timing. Since the PAW always move in a low speed, 0.1s delay will not cause a large effect on the overall system, the simulation result shown in Figure 30(b) still shows a good performance to estimate the human input timing.

6.3 Experiments

Several experiments are carried out to vertify the proposed method to estimate the human input timing. The experimental results are shown in Figure 31(c). The color code of each line is same as that of Figure 31. The threshold is set as 2.2. It can be seen from the Figure 31(a) and 31(b) that the proposed method can estimate the start of human input timing well, but when the human input ends, this method have about 0.5s delay. Figure 31(c) is the failure example of the proposed method, this is because some other disturbance exsists. About 70%

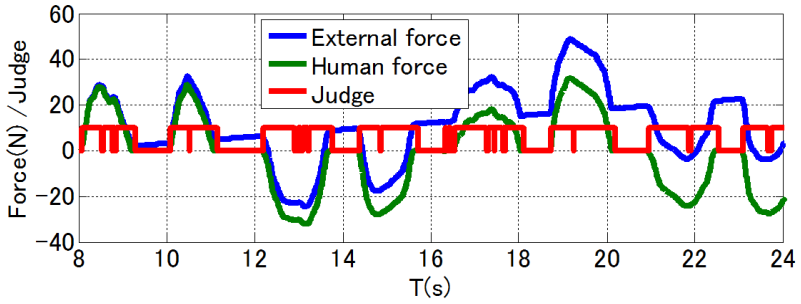

(a) Before improved.

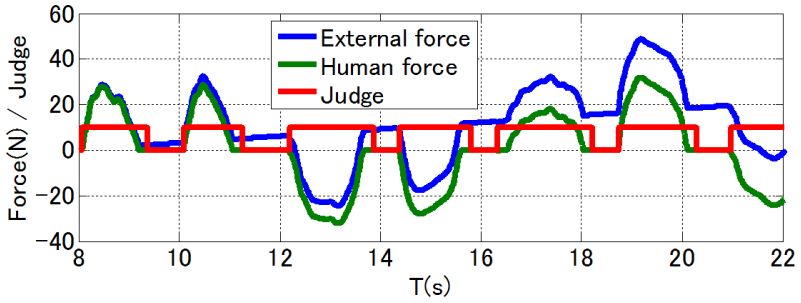

(b) After improved.

Figure 30: Human input timing estimation (Simulations)

of the experiments show good performance just like Experiment 1 and 2, about 30% of the experiments failed.

6.4 Conclusion

In this chapter, a method using different changing rate of human force and the disturbance is used to estimate human input timing. This method will cause some delay especially when the human input ends. Therefore, it need to be improved in the future. This method can be used in various environments if the condition that the human force changes much faster than other force is satisfied. However the threshold is very difficult to design, that is because the external force estimated from the DOB is not always correct especially when there is no human input.

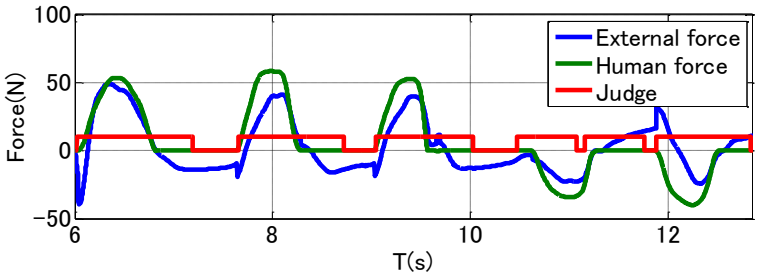

(a) Experiment 1.

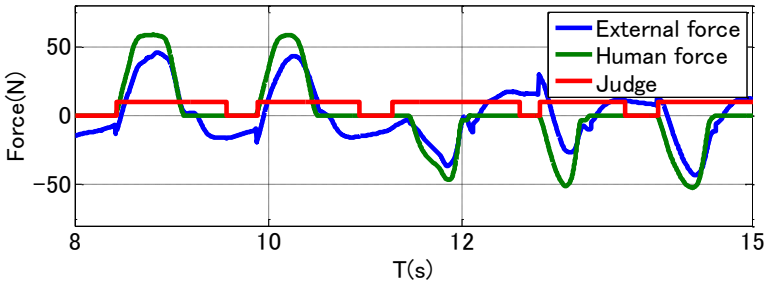

(b) Experiment 2.

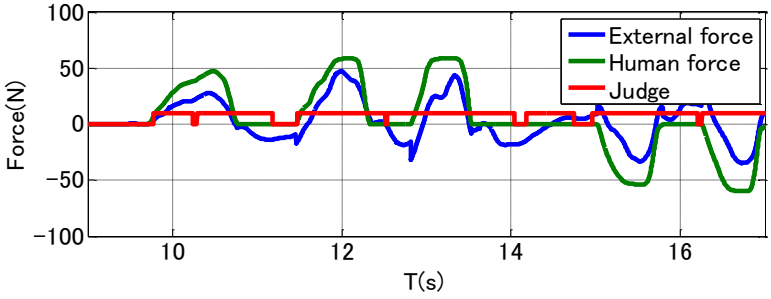

(c) Experiment 3.

Figure 31: Human input timing estimation (Experiments)

Chapter 7

Conclusion

In this paper, three basic methods to estimate human intention (human input force, human input timing) are proposed.

This paper can be divided into four parts. The first part is the modeling method for PAW considering the lateral and the longitudinal directions. The motion of PAW is divided into two portions: the common component and the differential component. The control system can be designed independently to meet the different need for users. When designing the power assist gains, the gains for straight (common component) and yaw (differential component) can be designed independently.

Secondly, the Fore Sensorless Power Assist Control system is applied in the PAW system. Using this control method instead of force sensors, the heavy and expensive force sensors will not be necessary.

Thirdly, three methods are proposed to extract human intention. Human force estimation considering the caster effects is introduced in Section four. Separating human force from the external force using the Recursive Least Square with Multiple Forgetting is introduced in Section five. Extraction human input timing using the different changing rate of human force and the disturbance is introduced in Section Six. Actually, the method introduced in Section four can be concluded that the human input can be obtained by removing the modeled disturbance. Section five and six introduce the methods which use different characteristics of human input and disturbance to extract the human intention. The author think these method can also be used in some other human-machine systems.

Lastly, the experimental methods is introduced. The devices which is used in this paper are firstly introduced. Then the experimental environments are introduced. The control algorithms can be realized because the PAW used in the experiments are refitted by increasing many sensors and S-box.

There are two main meanings for this research.

Firstly, by utilizing the DOB based estimator the external force can be obtained without the expensive and heavy force sensors. This can reduce the cast and the weight of the overall system.

Secondly, several methods are developed to extract human intention. The proposed methods are validated by simulations and experiments.

Acknowledgment

Two years ago, I sent an Email to Professor Hori inquiring the possibility to carry out my master course study at his lab. Professor Hori kindly gave me the chance to take the entrance examination. After entering the master course, with his patient guidance, kindly encouragement and critical critiques, I was able to accomplish this research and realize this dissertation. Not only on my research, Professor Hori also taught me a lot on how a good research and a man should be. Here, I want to express my infinite and deepest gratitude to Professor Hori.

I also want to thank Professor Fujimoto, he gave me a lot of advice in the report meeting. He always gave his first priority to his students.

Meanwhile, I want to thank all of the members in Hori-Fujimoto Lab. Thanks all for the discussion about the research, caring of my life. I would like to thank Dr. Kayoung for her kind help with my research.

Finally, I want to thank my family. They really gave me a lot of support when I met some difficulties.

Reference

[1] Ministry of Health, Labour and Welfare: policy report, Residence of the elderly, 3 (2009)

[2] 総務省統計局 (公式ホームページ), 人口推定（平成 26 年 10 月 1 日現在）: http://www.stat.go.jp/data/jinsui/2014np/index.htm

[3] Int.Home Care & Rehabilitation: 保険福祉 News2008, No.8 平成 22 年 11 月 27 日発行第 22 巻 (2008)

[4] K. A. Curtis, G. A. Drysdale, R. D. Lanza, M. Kolber, R. S. Vitolo,and R. West:“ Shoulder pain in wheelchair users with tetraplegia and paraplegia ”, Arch. Phys. Med. Rehabil., Volume: 80, No. 4, pp.453-457 (1999-4)

[5] Rory A. Cooper, Thomas A. Corfman, Shirley G. Fitzgerald, Michael L. Boninger, Donald M. Spaeth, William Ammer, and Julianna Arva:“ Performance Assessment of a Pushrim-Activated Power-Assisted Wheelchair Control System ”, IEEE Transactions on Control Systems and Technology, Volume:10, No.1,pp.121-126 (2002-1)

[6] Sehoon Oh, Naoki Hata, Yoichi Hori:“ Integrated Motion Control of a Wheelchair in the Longitudinal, Lateral, and Pitch Directions ”,Industrial Electronics, IEEE Transactions on Volume:55 , Issue: 4, pp.1855-1862 (2008-4)

[7] Kayoung Kim, K. Nam, S. Oh, H. Fujimoto, Y. Hori:“ Yaw Motion Control of Power-assisted Wheelchairs under Lateral Disturbance Environment ”,The 37th Annual Conf. of the IEEE Industrial Electronics Society, pp. 4111-4116, (2011-11).

[8] Kayoung Kim,Kanghyun Nam, Sehoon Oh, H. Fujimoto, Y. Hori:“ Two dimensional Assist Control for Power-assisted Wheelchair considering Straight and Rotational Motion Decomposition ”,IECON 2012 - 38th Annual Conference on IEEE Industrial Electronics Society,25-28,pp.4436-4441 (2012-10)

[9] Kazuki Takahashi, Hirokazu Seki and Susumn Tadakuma:“ Safety Driving Control for Electric Power Assisted Wheelchair Based On Regenerative Brake ”, Industrial Electronics, IEEE Trans, Volume: 56 , No.5,pp.1393 - 1400 (2009)

[10] Tsuyoshi SHIBATA,Toshiyuki MURAKAMI:“ Power Assist Control by Repulsive Compliance Control of Electric Wheelchair ”,Advanced Motion Control, 2008. AMC ’08. 10th IEEE International Workshop on Trento,26-28, pp.504-509 (2008-3)

[11] Tashiro, S, Yokohama; Murakami, T:“ Step Passage Control of a Power-Assisted Wheelchair for a Caregiver ”, Industrial Electronics, IEEE Transactions on (Volume:55 , Issue: 4) pp.1715-1721 (2008-4)

[12] T. Umeno and Y. Hori:“ Robust speed control of DC servomotors using modern two degrees-of-freedom controller design ”. IEEE Trans. Ind. Electron., vol. 38, no. 5, pp.363-368 (1991-10)

[13] Naoki Oda and Shouhei Mabuchi:“ Power Assisting Control with Visual Interaction for Robotic Wheelchair ”. The 2010 International Power Electronics Conference in Sapporo. pp.2210 - 2215 (2010-6)

[14] Sehoon Oh and Yoichi Hori:“ Generalized Discussion on Design of Force-sensor-less Power Assist Control ”. IEEE International Workshop on Advanced Motion Control in Trento. pp.492 - 497 (2008-3)

[15] Sehoon Oh, Kyoungchul Kong, and Yoichi Hori:“ Design and Analysis of Force-Sensor-Less Power-Assist Control ”.IEEE Transactions on Industrial Electronics. Volume: 61, Issue 2, pp.985-993 (2014-2)

[16] Junichi Miyata, Yukiko Kaida, and Toshiyuki Murakami:“ $v-\dot{\phi}$-Coordinate-Based Power-Assist Control of Electric Wheelchairs for a Caregiver ”. IEEE Transactions on Industrial Electronics. Volume: 55, No 6, pp.2517-2524 (2008-6)

[17] Rory A. Cooper,Carmen P. DiGiovine,Michael L. Boninger, Sean D. Shimada, Alicia M. Koontz, Mark A. Baldwin:“ Filter frequency selection for manual wheelchair biomechanics ”, Journal of rehabilitation research and development,Volume. 39 No. 3, pp.323-336 (2002-6)

[18] Carmen P. DiGiovine, Rory A. CooperFrequency:“ Analysis of Kinematics of Racing Wheelchair Propulsion ”, Transaction on Rehabilitation engineering. pp. 385-393 (2000)

[19] Yun X, Yamamoto Y:“ Internal dynamics of a wheeled mobile robot ”.IEEE/RSJ international conference on intelligent robots and systems; pp. 1288 (1993-7)

[20] Se-Han Lee and Jae-Bok Song:“ Acceleration estimator for low-velocity and low-acceleration regions based on encoder position data ”, Mechatronics, IEEE/ASME Transactions on Volume:6, Issue:1,pp.58-64 (2011-3)

[21] Barry W. Johnson, James H. Aylor:“ Dynamic Modeling of an Electric Wheelchair ”, IEEE Transactions on Industry Applications. Volume. 1A-21. No.5. pp.1284-1293 (1985-9)

[22] Dan Ding, Member,Rory A. Cooper, Songfeng Guo, and Thomas A. Corfman:“ Analysis of Driving Backward in an Electric-Powered Wheelchair ”, IEEE Transactions on Control Systems and Technology, Volume:12, No.6,pp.934-943 (2004-11)

[23] Chenier, F., Ecole de Technol. Super. de Montreal; Bigras, P.; Aissaoui, R:“ An Orientation Estimator for the Wheelchair's Caster Wheels ”, Control Systems Technology, IEEE Transactions on Volume:19, Issue:6, pp.1317-1326 (2011-11)

[24] K. Ogata, Modern Control Engineering. Upper Saddle River, NJ: Prentice-Hall, 1996.

[25] A. Vahidi , A. Stefanopoulou H. Peng:“ Recursive least squares with forgetting for online estimation of vehicle mass and road grade: theory and experiments ”, Vehicle System Dynamics: International Journal of Vehicle Mechanics and Mobility, 43:1, 31-55, DOI: 10.1080/00423110412331290446 (2005-1)

[26] A. Osorio Cordero, D.Q. Mayne:“ Deterministic convergence of a self-tuning regulator with variable forgetting factor ”, IEE Proceedings D on Control Theory and Applications, Volume:128 , Issue: 1. pp.19-23 (1981-1)

Publications

[1]	Authors	Lele XI (The University of Tokyo, Student of Master course)
		Yoichi HORI (The University of Tokyo, Professor)
	Theme	"Force Sensorless Power Assist Control for Wheelchairs Considering Caster Effects"
	Conference	Technical Committee on Mechatronics Control
	Place	Tokyo （Shibaura Institute of Technology ）
	Year Month	December, 2015

[2]	Authors	Lele XI (The University of Tokyo, Student of Master course)
		Yoichi HORI (The University of Tokyo, Professor)
	Theme	"Force Sensorless Power Assist Control for Wheelchair on Flat Road Using Recursive Least Square with Multiple Forgetting"
	Conference	IEEJ international workshop on Sensing, Actuation, Motion Control, and Optimization ,(SAMCON2016)
	Place	Tokyo, Japan
	Year Month	March, 2016(to be presented)